

Bayesian Smoothed Quantile Regression

Bingqi Liu* Kangqiang Li† Tianxiao Pang‡

School of Mathematical Sciences, Zhejiang University, Hangzhou 310058, China

Abstract

Bayesian quantile regression based on the asymmetric Laplace distribution (ALD) likelihood suffers from two fundamental limitations: the non-differentiability of the check loss precludes gradient-based Markov chain Monte Carlo (MCMC) methods, and the posterior mean provides biased quantile estimates. We propose Bayesian smoothed quantile regression (BSQR), which replaces the check loss with a kernel-smoothed version, creating a continuously differentiable likelihood. This smoothing has two crucial consequences: it enables efficient Hamiltonian Monte Carlo sampling, and it yields a consistent posterior distribution, thereby resolving the inferential bias of the standard approach. We further establish conditions for posterior propriety under various priors (including improper and hierarchical) and characterize how kernel choice affects posterior concentration and computational efficiency. Extensive simulations validate our theoretical findings, demonstrating that BSQR achieves up to a 50% reduction in predictive check loss at extreme quantiles compared to ALD-based methods, while improving MCMC efficiency by 20–40% in effective sample size. An empirical application to financial risk measurement during the COVID-19 era illustrates BSQR’s practical advantages in capturing dynamic systemic risk. The BSQR framework provides a theoretically-grounded and computationally-efficient solution to longstanding challenges in Bayesian quantile regression, with compact-support kernels like the uniform and triangular emerging as particularly effective choices.

Keywords: Bayesian inference; Hamiltonian Monte Carlo; Kernel smoothing; Posterior propriety; Quantile regression

MSC2020: Primary: 62F15, 62G08; Secondary: 62E20, 62P20

JEL Classification: Primary: C21; Secondary: C11, C14

*Corresponding author, E-mail: bqliu@zju.edu.cn (Bingqi Liu), ORCID: 0000-0003-0948-8930.

†E-mail: 11935023@zju.edu.cn (Kangqiang Li), ORCID: 0000-0002-4253-6730.

‡E-mail: txpang@zju.edu.cn (Tianxiao Pang).

Contents

1	Introduction	3
2	The Bayesian smoothed quantile regression framework	5
2.1	Motivation: The challenge of non-smoothness in Bayesian quantile inference	5
2.2	Technical foundation: Kernel smoothing of the check loss	6
2.3	The BSQR likelihood and posterior	7
3	Asymptotic posterior consistency	8
4	Posterior propriety under various prior specifications	9
4.1	Propriety with an improper uniform prior for β	9
4.2	Propriety with proper priors for β	10
5	Theoretical analysis of kernel selection in BSQR	12
5.1	Implications of kernel selection	12
5.2	Kernel effects on posterior concentration	14
6	Bayesian inference via MCMC	16
6.1	Hamiltonian Monte Carlo sampling for β	17
6.1.1	Gaussian kernel	18
6.1.2	Uniform kernel	19
6.1.3	Epanechnikov kernel	19
6.1.4	Triangular kernel	19
6.2	Metropolis-Hastings sampling for θ	20
7	Simulation	22
8	Empirical analysis: Asymmetric systemic risk exposure in the post-COVID era	24
8.1	Inferential stability and economic insights from asymmetric betas	25
8.2	Predictive accuracy and sampler efficiency	26
9	Discussion	28
References		29
Appendix A: Proofs		33
Appendix B: Algorithms		43

Appendix C: Derivations	45
C.1 Gaussian kernel	46
C.2 Uniform kernel	47
C.3 Epanechnikov kernel	48
C.4 Triangular kernel	49
Appendix D: Simulation results	51

1 Introduction

Quantile regression (QR), pioneered by [Koenker and Bassett \(1978\)](#), provides a comprehensive framework for modeling the conditional distribution of a response variable. Unlike ordinary least squares (OLS), which focuses only on the conditional mean, QR offers a robust characterization of distributional heterogeneity, driving its widespread adoption in fields from economics ([Chernozhukov et al., 2013](#)) to public health ([Koenker, 2005](#); [Hao & Naiman, 2007](#)). Foundational theory for QR is well-established ([Portnoy, 1984](#); [Knight, 1998](#)), and the framework has been extended to handle complex scenarios including nonparametric settings ([Koenker et al., 1994](#); [Yu & Jones, 1998](#)) and high-dimensional data ([Belloni & Chernozhukov, 2011](#)).

The Bayesian paradigm offers unique advantages for QR, including coherent uncertainty quantification and flexible model construction. The key breakthrough for Bayesian quantile regression (BQR) was the discovery that minimizing the check loss function is equivalent to maximizing a likelihood based on the asymmetric Laplace distribution (ALD) ([Yu & Moyeed, 2001](#)). This insight, combined with a scale-mixture-of-normals representation that enables efficient Gibbs sampling ([Kozumi & Kobayashi, 2011](#)), catalyzed the development of a rich BQR literature, including methods for variable selection ([Li et al., 2010](#); [Alhamzawi & Ali, 2018](#)) and applications to complex data structures ([Reich et al., 2011](#); [Geraci & Bottai, 2007](#)).

Despite its success, the standard ALD-based BQR framework is hamstrung by two fundamental limitations. First, its use of the non-differentiable check loss function, $\rho_\tau(u) = u(\tau - \mathbb{I}(u < 0))$, precludes the application of modern gradient-based samplers like Hamiltonian Monte Carlo (HMC) and the No-U-Turn sampler (NUTS) ([Neal, 2011](#); [Hoffman & Gelman, 2014](#)). These algorithms represent a paradigm shift in Bayesian computation, offering dramatic gains in sampling efficiency, especially in high-dimensional and correlated settings ([Betancourt, 2017](#); [Livingstone & Zanella, 2019](#)). Consequently, BQR practitioners are relegated to less efficient Gibbs samplers that can suffer from slow convergence. Second, the inferential target is misaligned: while the posterior mode under the ALD likelihood corresponds to the frequentist QR estimate, the posterior mean — the standard Bayesian point estimate — is a biased

estimator of the true conditional quantile and does not minimize the expected check loss (Sriram et al., 2013; Yang et al., 2016). This is a critical flaw, as the check loss is the unique proper scoring rule for evaluating quantile forecasts (Gneiting, 2011).

The idea of smoothing the check loss to enable gradient-based methods has a rich history in frequentist QR (Horowitz, 1998), with recent theoretical work showing that smoothed estimators can achieve the same asymptotic efficiency as their non-smooth counterparts (Fernandes et al., 2021). However, these powerful ideas have not been systematically developed for Bayesian inference, representing a significant gap in the literature.

This paper introduces Bayesian smoothed quantile regression (BSQR) to fill this gap, proposing a framework that resolves both limitations through a principled reformulation of the likelihood. Our key innovation is to replace the non-smooth check loss with a kernel-smoothed version, $L_h(\cdot; \tau) = \int_{-\infty}^{\infty} \rho_{\tau}(\cdot - v) K_h(v) dv$, creating a continuously differentiable objective function. The foundation of our approach is to then construct a likelihood directly from this smoothed loss. We propose a novel error distribution whose probability density is proportional to the exponentiated negative smoothed loss, taking the form $f_{\text{SQR}}(\cdot) \propto \exp(-\theta L_h(\cdot; \tau))$, where $\theta > 0$ is a scale parameter. This construction, formally detailed in Section 2.3, ensures that the entire Bayesian inferential machinery is coherently aligned with the smoothed quantile objective.

The contributions of this paper are fivefold. First, we establish the asymptotic posterior consistency of BSQR, formally resolving the inferential bias of the ALD-based approach. Second, we develop conditions for posterior propriety under various priors and show that our framework converges to standard BQR as the smoothing bandwidth $h \rightarrow 0$. Third, we provide a rigorous analysis of kernel selection and its impact on posterior inference. Fourth, we develop efficient HMC and NUTS algorithms that fully exploit the smoothed likelihood. Fifth, through extensive simulations and an empirical application, we demonstrate that BSQR yields superior predictive accuracy and computational efficiency compared to standard BQR. To facilitate reproducibility and promote further research, the complete source code for all numerical experiments is publicly available in a dedicated repository.¹

The remainder of this paper is organized as follows. Section 2 presents the BSQR model. Sections 3, 4, and 5 establish its core theoretical properties. Section 6 details the computational framework. Sections 7 and 8 present simulation evidence and an empirical application. Section 9 concludes. All proofs, technical derivations, and the simulation results tables are provided in the appendices.

¹The replication package is available at <https://github.com/BeauquinLau/BSQR>.

2 The Bayesian smoothed quantile regression framework

This section develops the BSQR framework. We begin by motivating the need for a new approach, rooted in the fundamental limitations of standard BQR. We then lay out the technical foundations for loss smoothing, drawing from the frequentist literature, before constructing our novel, principled Bayesian model upon this foundation.

2.1 Motivation: The challenge of non-smoothness in Bayesian quantile inference

The linear QR model specifies the τ -th conditional quantile of a response variable Y as a linear function of covariates \mathbf{X} . We assume that observed pairs (y_i, \mathbf{x}_i) are independent and identically distributed (i.i.d.) samples from an underlying joint distribution (Y, \mathbf{X}) . For a given quantile level $\tau \in (0, 1)$, this relationship is:

$$Q_Y(\tau | \mathbf{x}_i) = \mathbf{x}_i^\top \boldsymbol{\beta}(\tau), \quad i = 1, \dots, n, \quad (1)$$

where $Q_Y(\tau | \mathbf{x}_i) := \inf\{q : F_{Y|\mathbf{X}}(q | \mathbf{x}_i) \geq \tau\}$ with $F_{Y|\mathbf{X}}(\cdot | \mathbf{x}_i)$ being the conditional cumulative distribution function (CDF) of Y given $\mathbf{X} = \mathbf{x}_i$, $\mathbf{x}_i \in \mathbb{R}^d$ is a covariate vector (including a constant term $x_{i1} = 1$ to accommodate an intercept), and $\boldsymbol{\beta}(\tau) \in \mathbb{R}^d$ is the coefficient vector. This implies that the error term, $\varepsilon_i(\tau) := y_i - \mathbf{x}_i^\top \boldsymbol{\beta}(\tau)$ (which for notational convenience we will henceforth write as ε_i), has a zero τ -th conditional quantile, $Q_\varepsilon(\tau | \mathbf{x}_i) = 0$. We adopt the standard assumption of independence between the covariates \mathbf{x}_i and the error term ε_i . This simplifies the quantile condition to the unconditional requirement $F_\varepsilon(0) = \tau$.

As established by [Koenker and Bassett \(1978\)](#), the population coefficient vector $\boldsymbol{\beta}(\tau)$ minimizes the expected check loss:

$$R(\mathbf{b}; \tau) := \mathbb{E} [\rho_\tau(\zeta)] = \int_{-\infty}^{\infty} \rho_\tau(e) dF_\zeta(e), \quad (2)$$

where $\zeta := Y - \mathbf{X}^\top \mathbf{b}$ represents the population-level residual corresponding to a candidate coefficient vector \mathbf{b} , $F_\zeta(e) := \Pr[\zeta \leq e]$, and $\rho_\tau(e) = e(\tau - \mathbb{I}(e < 0))$ is the non-differentiable ‘pinball’ loss function. The sample estimator, $\hat{\boldsymbol{\beta}}(\tau)$, is found by minimizing its empirical counterpart:

$$\hat{R}(\mathbf{b}; \tau) := \frac{1}{n} \sum_{i=1}^n \rho_\tau(e_i(\mathbf{b})), \quad (3)$$

where $e_i(\mathbf{b}) := y_i - \mathbf{x}_i^\top \mathbf{b}$ denotes the residual for the i -th observation under a candidate parameter vector \mathbf{b} .

The Bayesian quantile regression (BQR) paradigm connects to this objective via the ALD, whose probability density function (PDF) is $p_{\text{ALD}}(\cdot; \theta, \tau) \propto \exp(-\theta \rho_\tau(\cdot))$ ([Yu & Moyeed, 2001](#)). While this

formulation ensures that its posterior mode, which we denote $\check{\beta}$, numerically coincides with the frequentist point estimator $\hat{\beta}(\tau)$, this reliance on the non-smooth check loss imposes critical limitations: it precludes the use of modern gradient-based samplers (e.g., HMC) and creates a misalignment between the posterior mean and the true quantile, the latter being the target of the proper check loss scoring rule (Sriram et al., 2013; Gneiting, 2011). These challenges motivate a fundamental reformulation of the Bayesian likelihood.

2.2 Technical foundation: Kernel smoothing of the check loss

The key to overcoming non-differentiability lies in smoothing the loss function, an idea explored in the frequentist SQR literature (Horowitz, 1998; Fernandes et al., 2021). The approach begins by replacing the discrete empirical CDF of residuals with a kernel-smoothed version. Let $K(\cdot)$ be a symmetric kernel with bandwidth $h > 0$, and $K_h(v) = h^{-1}K(v/h)$. The SQR objective is formulated via a Stieltjes integral over the smoothed residual CDF, $\widehat{F}_h(t)$:

$$\widehat{R}_h(\mathbf{b}; \tau, h) := \int_{-\infty}^{\infty} \rho_{\tau}(t) d\widehat{F}_h(t), \quad \text{where } \widehat{F}_h(t) = \int_{-\infty}^t \left(\frac{1}{n} \sum_{i=1}^n K_h(v - e_i(\mathbf{b})) \right) dv. \quad (4)$$

Building upon this, we show that the integral can be re-expressed in a more analytically tractable form. By expanding the definition of $d\widehat{F}_h(t)$, we arrive at:

$$\widehat{R}_h(\mathbf{b}; \tau, h) = \frac{1}{n} \sum_{i=1}^n \int_{-\infty}^{\infty} \rho_{\tau}(t) K_h(t - e_i(\mathbf{b})) dt = \frac{1}{n} \sum_{i=1}^n \int_{-\infty}^{\infty} \rho_{\tau}(v + e_i(\mathbf{b})) K_h(v) dv, \quad (5)$$

where the second equality follows from the change of variables $v = t - e_i(\mathbf{b})$. This derivation motivates our definition of a *smoothed check loss function*:

$$\begin{aligned} L_h(e; \tau) &:= \int_{-\infty}^{\infty} \rho_{\tau}(v + e) K_h(v) dv = \int_{-\infty}^{\infty} \rho_{\tau}(w) K_h(w - e) dw \\ &= \int_{-\infty}^{\infty} \rho_{\tau}(w) K_h(e - w) dw = (\rho_{\tau} * K_h)(e). \end{aligned} \quad (6)$$

This function, the convolution of the check loss with the kernel, allows the SQR objective to be written compactly as an average smoothed loss, whose minimizer is the SQR estimator $\hat{\beta}_h(\tau)$:

$$\widehat{R}_h(\mathbf{b}; \tau, h) = \frac{1}{n} \sum_{i=1}^n L_h(e_i(\mathbf{b}); \tau), \quad \text{where } \hat{\beta}_h(\tau) := \arg \min_{\mathbf{b} \in \mathbb{R}^d} \widehat{R}_h(\mathbf{b}; \tau, h). \quad (7)$$

A key advantage of this formulation is its inherent differentiability. The derivative of the smoothed loss, denoted as $\Psi_h(e; \tau)$, is the convolution of the check loss subderivative $\psi_{\tau}(e) = \tau - \mathbb{I}(e < 0)$ ² with the kernel:

$$\Psi_h(e; \tau) := \frac{\partial L_h(e; \tau)}{\partial e} = (\psi_{\tau} * K_h)(e) = \int_{-\infty}^{\infty} \psi_{\tau}(e - v) K_h(v) dv. \quad (8)$$

²Strictly speaking, $\psi_{\tau}(e) = \tau - \mathbb{I}(e < 0)$ is a subderivative, as $\rho_{\tau}(e)$ is non-differentiable at $e = 0$ due to the discontinuity in ψ_{τ} . However, this non-differentiability does not affect the subsequent smoothing and computation, as the convolution with a sufficiently smooth kernel K_h yields a differentiable Ψ_h .

As shown in Eq. (18), this simplifies to a clean form using the kernel's CDF, $F_K(\cdot)$:

$$\Psi_h(e; \tau) = F_K\left(\frac{e}{h}\right) - (1 - \tau). \quad (9)$$

This analytical gradient is fundamental to the efficient application of HMC methods for Bayesian inference, as detailed in Section 6.

2.3 The BSQR likelihood and posterior

Standard BQR, based on the ALD, does not target the SQR estimator $\hat{\beta}_h(\tau)$ because $L_h(e; \tau) \neq \rho_\tau(e)$. To establish a Bayesian framework that is both computationally efficient and inferentially coherent with the smoothed objective, we propose a novel likelihood constructed directly from first principles. The core of our BSQR model is a new error distribution, f_{SQR} , whose negative log-density is defined to be proportional to the smoothed check loss itself:

$$f_{\text{SQR}}(\varepsilon; \theta, \tau, h) = \frac{1}{Z(\theta, \tau, h)} \exp(-\theta L_h(\varepsilon; \tau)), \quad (10)$$

where $\theta > 0$ is a scale parameter, and $Z(\theta, \tau, h)$ is the normalizing constant required for f_{SQR} to be a valid PDF:

$$Z(\theta, \tau, h) := \int_{-\infty}^{\infty} \exp(-\theta L_h(u; \tau)) \, du. \quad (11)$$

Denote the observed dataset $\mathbf{y} = (y_1, \dots, y_n)$ and $\mathbf{X} = (\mathbf{x}_1^\top, \dots, \mathbf{x}_n^\top)^\top$, then the joint likelihood for (\mathbf{y}, \mathbf{X}) given the parameters β and θ is:

$$L(\mathbf{y} | \mathbf{X}, \beta, \theta; \tau, h) = \prod_{i=1}^n f_{\text{SQR}}(e_i(\beta); \theta, \tau, h) = \left(\frac{1}{Z(\theta, \tau, h)} \right)^n \exp\left(-\theta \sum_{i=1}^n L_h(e_i(\beta); \tau)\right). \quad (12)$$

The corresponding log-likelihood is therefore:

$$\ell(\mathbf{y} | \mathbf{X}, \beta, \theta; \tau, h) = -n \log Z(\theta, \tau, h) - \theta \sum_{i=1}^n L_h(e_i(\beta); \tau). \quad (13)$$

By this construction, maximizing the log-likelihood with respect to β is equivalent to minimizing the SQR objective function in Eq. (7). This establishes a direct and principled link between our Bayesian model and the SQR estimator. Completing the model requires specifying priors for β and θ . Assuming prior independence, such that $\pi(\beta, \theta) = \pi(\beta)\pi(\theta)$, the posterior distribution follows from Bayes' theorem:

$$\pi(\beta, \theta | \mathbf{y}, \mathbf{X}; \tau, h) \propto L(\mathbf{y} | \mathbf{X}, \beta, \theta; \tau, h) \pi(\beta)\pi(\theta)$$

³The interchange of differentiation and integration is justified by the dominated convergence theorem. The partial derivative of the integrand with respect to e , namely $\psi_\tau(e - v)K_h(v)$, is bounded in absolute value by $\max(\tau, 1 - \tau)K_h(v)$. This dominating function is integrable over $v \in \mathbb{R}$ since K_h is a probability density, thus satisfying the conditions for the theorem.

$$\propto (Z(\theta, \tau, h))^{-n} \exp \left(-\theta \sum_{i=1}^n L_h(e_i(\beta); \tau) \right) \pi(\beta) \pi(\theta). \quad (14)$$

While this formulation enables efficient gradient-based sampling (see Section 6), its most critical theoretical virtue lies in its large-sample behavior. As we formally establish in Section 3, this posterior is consistent for the true quantile parameters, rectifying a known inferential bias in standard BQR.

3 Asymptotic posterior consistency

A foundational theoretical question for any Bayesian model is whether its posterior distribution concentrates around the true parameter value as the sample size increases. This property, known as posterior consistency, is particularly crucial for our proposed BSQR framework. As highlighted by [Sriram et al. \(2013\)](#), the posterior mean derived from the standard ALD-based BQR is not a consistent estimator of the true conditional quantile parameter. This section formally establishes that the BSQR posterior is consistent, providing the theoretical justification that our estimator indeed targets the correct parameter in large samples and thus resolves the inferential bias of the standard approach.

Assumption 1 (Regularity conditions for consistency). *Let the true data generating process be governed by a linear conditional quantile model, such that $Q_Y(\tau \mid \mathbf{x}_i) = \mathbf{x}_i^\top \beta_0(\tau)$, where $\beta_0(\tau)$ is the true parameter vector. Define the error term as $\varepsilon_{0i} = y_i - \mathbf{x}_i^\top \beta_0(\tau)$. By construction, the τ -th conditional quantile of ε_{0i} given \mathbf{x}_i is zero, which implies that $F_{\varepsilon_0}(0) = \tau$. This outcome is similar to that in Eq. (1). The following conditions are assumed to hold:*

(C1) Parameter Space: *The parameter space \mathcal{B} for $\beta(\tau)$ is a compact subset of \mathbb{R}^d , with the true parameter $\beta_0(\tau)$ in its interior.*

(C2) Error Distribution: *The error term ε_{0i} satisfies the following:*

(a) *The CDF $F_{\varepsilon_0}(\cdot)$ is at least twice continuously differentiable in a neighborhood of 0, with a PDF $f_{\varepsilon_0}(\cdot) = F'_{\varepsilon_0}(\cdot)$ that is positive at 0, i.e., $f_{\varepsilon_0}(0) > 0$.*

(b) *The first moment of the error is finite, i.e., $\mathbb{E}[|\varepsilon_{0i}|] < \infty$.*

(C3) Covariates: *The covariate vectors \mathbf{x}_i are i.i.d. and uniformly bounded. The sample second moment matrix converges in probability to a positive definite matrix Σ_X as $n \rightarrow \infty$, i.e., $n^{-1} \sum_{i=1}^n \mathbf{x}_i \mathbf{x}_i^\top \xrightarrow{P} \Sigma_X$.*

(C4) Kernel Properties: *The kernel function $K(\cdot)$ is a symmetric, bounded PDF satisfying $\int_{-\infty}^{\infty} u K(u) \, du = 0$ and $\int_{-\infty}^{\infty} u^2 K(u) \, du < \infty$.*

(C5) Prior Distribution: The prior distribution $\pi(\beta)$ is continuous and assigns positive probability to any open neighborhood of the true parameter $\beta_0(\tau)$.

Theorem 1 (Posterior consistency of BSQR). *Under Assumption 1, the posterior distribution $\pi(\beta | \mathbf{y}, \mathbf{X}, \theta)$ derived from the smoothed likelihood in Eq. (12) is consistent at the true parameter value $\beta_0(\tau)$. That is, for any neighborhood U of $\beta_0(\tau)$,*

$$\int_U \pi(\beta | \mathbf{y}, \mathbf{X}, \theta) d\beta \xrightarrow{P} 1 \quad \text{as } n \rightarrow \infty,$$

where the convergence is in probability with respect to the true data generating distribution.

The proof of this theorem is provided in [Appendix A](#).

[Theorem 1](#) forms the theoretical cornerstone of our BSQR framework, establishing posterior consistency and thereby addressing the known inconsistency of standard BQR estimators. The result hinges on the symmetrizing property of our smoothing procedure: By convolving the asymmetric check loss with a symmetric kernel, the resulting objective function becomes asymptotically unbiased in expectation, as captured in the proof's pivotal step where $\mathbb{E}[\Psi_h(\varepsilon_{0i}; \tau)] \rightarrow 0$. This guarantee ensures that, in large samples, BSQR inferences — such as posterior means and credible intervals — are centered on the true parameters, providing a foundation for the simulation results in Section 7 and explaining BSQR's superior out-of-sample performance relative to biased BQR-ALD, particularly at extreme quantiles.

4 Posterior propriety under various prior specifications

In this section, we investigate the propriety of the posterior distribution for the BSQR model parameters under several common prior choices for the regression coefficients β and the scale parameter θ . We begin by analyzing the case of an improper uniform prior for β , then extend this to a prior distribution, and finally consider hierarchical prior structures. Throughout this section, we assume the likelihood function for the BSQR model is given by Eq. (12), and we denote $S(\beta; \tau, h) = \sum_{i=1}^n L_h(y_i - \mathbf{x}_i^\top \beta; \tau) = \sum_{i=1}^n L_h(e_i(\beta); \tau)$.

4.1 Propriety with an improper uniform prior for β

Our investigation into posterior propriety commences with an examination of the posterior under an improper uniform prior for the regression coefficients, $\pi(\beta) \propto 1$. Its use here is particularly insightful as it allows us to isolate the influence of the likelihood term on posterior integrability, distinct from the regularizing effects that would be introduced by a proper prior for β . We first analyze the case with fixed θ to establish baseline propriety conditions, then generalize to complex settings by assigning θ a prior distribution. The following theorem establishes these propriety conditions, while its proof is deferred to [Appendix A](#).

Theorem 2 (Propriety under improper uniform prior for β). *Let the kernel function $K(\cdot)$ be non-negative, integrate to unity, and possess a finite first absolute moment (i.e., $\int_{-\infty}^{\infty} |u|K(u) du < \infty$). Separately, assume the $n \times d$ design matrix \mathbf{X} has full column rank d and $\pi(\beta) \propto 1$.*

(i) (Fixed θ) *If the scale parameter $\theta > 0$ is fixed, then the posterior distribution of β , $\pi(\beta | \mathbf{y}, \mathbf{X}, \theta)$, is proper. Equivalently,*

$$0 < \int_{\mathbb{R}^d} L(\mathbf{y} | \mathbf{X}, \beta, \theta; \tau, h) \pi(\beta) d\beta < \infty.$$

(ii) (Prior for θ) *If the scale parameter θ is assigned a prior distribution $\pi(\theta)$, then for a certain constant $C_S \geq 0$, the joint posterior distribution $\pi(\beta, \theta | \mathbf{y}, \mathbf{X})$ is proper if the integral*

$$\int_0^{\infty} \frac{\pi(\theta) e^{\theta C_S}}{(Z(\theta, \tau, h))^n \theta^d} d\theta \quad (15)$$

converges to a finite positive value. As a specific instance, if $\pi(\theta) \sim \text{Gamma}(a, b)$ with $a, b > 0$, and further assuming that $L_h(u; \tau)$ is twice continuously differentiable and attains its global minimum $L_{\min} = \min_u L_h(u; \tau)$ at a unique point u_{\min} where $L_h''(u_{\min}; \tau) > 0$, the posterior is proper if $b > C_S + nL_{\min}$ and $a + k_Z > d$, where $k_Z \geq 0$ is a constant such that $(Z(\theta, \tau, h))^{-n} = O(\theta^{k_Z})$ as $\theta \rightarrow 0$.

Remark 1. For Theorem 2(ii), the condition $b > C_S + nL_{\min}$ for the Gamma prior hyperparameter b is a significant and insightful result of our analysis. Unlike standard conditions that are independent of the sample size, our finding reveals a crucial interplay between the prior specification (via b), the sample size (n), and the intrinsic properties of the smoothed loss function (via its minimum, L_{\min}). It mandates that the prior on θ must be increasingly informative (i.e., have a larger rate parameter b) as the sample size grows to ensure posterior propriety under an improper prior for β . This requirement stems from the powerful influence of the likelihood, where the sample size n appears as an exponent in the normalizing constant term $(Z(\theta, \tau, h))^{-n}$. The asymptotic behavior of this term for large θ , derived via Laplace's method as shown in the proof, is $(Z(\theta, \tau, h))^{-n} = O(\theta^{n/2} e^{n\theta L_{\min}})$. To ensure posterior integrability, the exponential decay of the Gamma prior, $e^{-b\theta}$, must dominate this exponential growth, which directly yields the condition $b > C_S + nL_{\min}$. The second condition, $a + k_Z > d$, is more conventional and addresses the behavior near $\theta = 0$, ensuring the prior guards against non-identifiability.

4.2 Propriety with proper priors for β

Having established conditions for posterior propriety under an improper uniform prior for β , we now transition to proper prior specifications, which often enhance model regularization and inferential robustness. Following a conventional practice in Bayesian modeling, many contemporary BQR methodologies (e.g., [Kozumi & Kobayashi, 2011](#); [Li et al., 2010](#)) also use the analytically convenient Gaussian

distribution as a prior for the regression coefficients. A common strategy is to specify a Gaussian prior with a sufficiently large variance, thereby emulating a weakly informative stance while preserving the mathematical advantages of a proper distribution, such as facilitating the establishment of posterior propriety under less restrictive conditions. These considerations lead us to [Theorem 3](#), whose proof is given in [Appendix A](#) and which establishes the conditions for posterior propriety when β is assigned such a Gaussian prior.

Theorem 3 (Propriety under Gaussian prior for β). *Let the kernel function $K(\cdot)$ be non-negative and integrate to unity, and the prior for β be Gaussian, $\pi(\beta | \sigma_\beta^2) = (2\pi\sigma_\beta^2)^{-d/2} \exp\left(-\frac{\|\beta\|_2^2}{2\sigma_\beta^2}\right)$, with a fixed prior variance $\sigma_\beta^2 > 0$.*

(i) (Fixed θ) *If the scale parameter $\theta > 0$ is fixed, the posterior distribution $\pi(\beta | \mathbf{y}, \mathbf{X}, \theta, \sigma_\beta^2)$ is proper. That is,*

$$0 < \int_{\mathbb{R}^d} L(\mathbf{y} | \mathbf{X}, \beta, \theta; \tau, h) \pi(\beta | \sigma_\beta^2) d\beta < \infty.$$

(ii) (Prior for θ) *If the scale parameter θ is assigned a proper prior distribution $\pi(\theta)$, then the joint posterior distribution $\pi(\beta, \theta | \mathbf{y}, \mathbf{X}, \sigma_\beta^2)$ is proper if the integral*

$$\int_0^\infty (Z(\theta, \tau, h))^{-n} \pi(\theta) d\theta$$

converges to a finite positive value. As a specific instance, if $\pi(\theta) \sim \text{Gamma}(\theta | a_\theta, b_\theta)$ with $a_\theta > 0$ and $b_\theta > 0$, the joint posterior $\pi(\beta, \theta | \mathbf{y}, \mathbf{X}, \sigma_\beta^2, a_\theta, b_\theta)$ is proper if

$$\int_0^\infty (Z(\theta, \tau, h))^{-n} \theta^{a_\theta-1} e^{-b_\theta\theta} d\theta$$

converges to a finite positive value.

Following the establishment of posterior propriety for a fixed prior variance σ_β^2 (as in [Theorem 3](#)), a natural progression in Bayesian modeling involves treating σ_β^2 as a random variable to enhance model flexibility and allow the data to inform its scale. This is achieved through a hierarchical approach where σ_β^2 is assigned its own hyperprior. A common and theoretically convenient choice for variance hyperpriors is the inverse Gamma distribution, due to its positive support and analytical tractability. Consequently, it becomes pertinent to examine the conditions ensuring the propriety of the resulting joint posterior distribution, which is addressed in the following corollary.

Corollary 1 (Propriety under hierarchical Gaussian prior for β). *Let the kernel $K(\cdot)$ be non-negative and integrate to unity. The prior for β is conditionally Gaussian: $\pi(\beta | \sigma_\beta^2) = (2\pi\sigma_\beta^2)^{-d/2} \exp\left(-\frac{\|\beta\|_2^2}{2\sigma_\beta^2}\right)$, and the hyperprior for σ_β^2 is Inverse-Gamma: $\pi(\sigma_\beta^2 | a_0, b_0) = \text{IG}(\sigma_\beta^2 | a_0, b_0)$ with $a_0 > 0$ and $b_0 > 0$.*

(i) (Fixed θ) If $\theta > 0$ is fixed, the marginal posterior distribution $\pi(\beta, \sigma_\beta^2 | \mathbf{y}, \mathbf{X}, \theta, a_0, b_0)$ is proper.

Equivalently,

$$0 < \int_0^\infty \int_{\mathbb{R}^d} L(\mathbf{y} | \mathbf{X}, \beta, \theta; \tau, h) \pi(\beta | \sigma_\beta^2) \pi(\sigma_\beta^2 | a_0, b_0) d\beta d\sigma_\beta^2 < \infty.$$

(ii) (Prior for θ) If the scale parameter θ is assigned a proper prior distribution $\pi(\theta)$, then the joint posterior distribution $\pi(\beta, \sigma_\beta^2, \theta | \mathbf{y}, \mathbf{X}, a_0, b_0)$ is proper if the integral

$$\int_0^\infty (Z(\theta, \tau, h))^{-n} \pi(\theta) d\theta$$

converges to a finite positive value. As a specific instance, if $\pi(\theta) \sim \text{Gamma}(\theta | a_\theta, b_\theta)$ with $a_\theta > 0$ and $b_\theta > 0$, the joint posterior $\pi(\beta, \sigma_\beta^2, \theta | \mathbf{y}, \mathbf{X}, a_0, b_0, a_\theta, b_\theta)$ is proper if

$$\int_0^\infty (Z(\theta, \tau, h))^{-n} \theta^{a_\theta-1} e^{-b_\theta \theta} d\theta$$

converges to a finite positive value.

Remark 2. The use of a proper Gaussian prior for β , even conditionally within a hierarchy, significantly simplifies propriety arguments. The likelihood term $\exp(-\theta S(\beta; \tau, h))$ being bounded above allows integrability to be largely determined by the priors for β and its variance parameters. When $\pi(\beta | \sigma_\beta^2)$ is Gaussian and $\pi(\sigma_\beta^2)$ is a proper PDF (like Inverse-Gamma), the overall integral typically converges without stringent conditions on the rank of \mathbf{X} or specific relationships between prior parameters and the dimension d .

5 Theoretical analysis of kernel selection in BSQR

In this section, we theoretically investigate the role of the kernel function $K(\cdot)$ in shaping the BSQR posterior distribution. Our analysis proceeds in two parts. First, we establish fundamental properties of the posterior, demonstrating that for any compact support kernel, the BSQR posterior for the regression coefficients is equivalent in its tail behavior to that of standard ALD-based BQR. Second, we explore the finer-grained impact of the kernel's shape, showing that more “peaked” kernels lead to a more concentrated posterior distribution. These results provide both a theoretical justification for our method and a principle for kernel selection.

5.1 Implications of kernel selection

Building upon the discussion of posterior propriety from Section 4, we now examine how the choice of the kernel function $K(\cdot)$ and the associated smoothed loss $L_h(\cdot; \tau)$ influences key characteristics of the BSQR posterior distribution (Eq. (14)). This subsection explores two such crucial properties. Firstly, we

investigate the behavior of the normalizing constant $Z(\theta, \tau, h)$ in the error distribution $f_{\text{SQR}}(\cdot; \theta, \tau, h)$ in Eq. (10). This constant is integral to the likelihood (Eq. (12)) and the Markov Chain Monte Carlo (MCMC) sampling of θ , making its properties with respect to θ particularly relevant. Secondly, we analyze the relationship between the BSQR posterior and the standard ALD-based QR posterior, specifically when compact support kernels are employed, to understand the implications of smoothing for inference on β .

Proposition 1 (Properties of $Z(\theta, \tau, h)$). *The function $Z(\theta, \tau, h)$, as defined in Eq. (11), is based on the smoothed loss $L_h(u; \tau)$ which is non-negative for all $u \in \mathbb{R}$ and not identically zero. Consequently, for fixed τ and h :*

- (i) $Z(\theta, \tau, h)$ is a strictly decreasing function of $\theta > 0$.
- (ii) $\log Z(\theta, \tau, h)$ is a convex function of $\theta > 0$.

The proof of this proposition is provided in [Appendix A](#).

Remark 3. *The convexity of $\log Z(\theta, \tau, h)$ with respect to θ has important consequences. Since $-n \log Z(\theta, \tau, h)$ is concave in θ and the term $-\theta \sum_{i=1}^n L_h(e_i(\beta); \tau)$ is linear (hence concave), the θ -dependent portion of the log-likelihood (Eq. (13)) is concave. If the prior $\pi(\theta)$ is also log-concave, the conditional log-posterior of θ , $\log \pi(\theta | \beta, \mathbf{y}, \mathbf{X}; \tau, h)$, is therefore also concave. Such log-concavity is highly beneficial, as these posteriors are often unimodal and well-behaved, improving MCMC sampling efficiency and convergence for θ .*

Another pertinent question is how the BSQR posterior, $\pi_{\text{BSQR}}(\beta | \theta, \mathbf{y}, \mathbf{X}; \tau, h)$, relates to the posterior derived from a standard ALD likelihood, $\pi_{\text{ALD}}(\beta | \theta, \mathbf{y}, \mathbf{X}; \tau)$, especially concerning their tail behaviors. When compact support kernels (e.g., Uniform, Epanechnikov, Triangular, with support normalized to $[-1, 1]$) are used in BSQR, the smoothed loss $L_h(e; \tau)$ coincides with the standard check loss $\rho_\tau(e)$ (up to an additive constant independent of e) when the absolute value of the scaled residual $|e/h|$ exceeds 1. This localizes the smoothing effect to residuals close to zero. This observation motivates investigating whether the two posteriors are *equivalent* in a specific sense.

We define the ALD-based likelihood as $L_{\text{ALD}}(\mathbf{y} | \mathbf{X}, \beta, \theta; \tau) \propto \exp(-\theta \sum_{i=1}^n \rho_\tau(e_i(\beta)))$, assuming an implicit normalizing constant for the ALD PDF that does not depend on β . The corresponding posterior is $\pi_{\text{ALD}}(\beta | \theta, \mathbf{y}, \mathbf{X}; \tau) \propto L_{\text{ALD}}(\mathbf{y} | \mathbf{X}, \beta, \theta; \tau) \pi(\beta)$. The following theorem formally establishes the nature of this equivalence under the condition that compact support kernels are used in the BSQR model. The complete proof appears in [Appendix A](#).

Theorem 4 (Posterior equivalence for BSQR with compact kernels). *Assume that the kernel $K(\cdot)$ has compact support, say $[a, b]$ for finite $a < b$, is symmetric around its mean⁴, then there exist positive*

⁴Specifically, $K(\cdot)$ is symmetric with respect to its mean $\mu_K := \int_{-\infty}^{\infty} u K(u) du$, meaning that $K(\mu_K + v) = K(\mu_K - v)$ for all v in the support. In the proof, we re-center the kernel to have zero mean for simplicity.

constants M_1 and M_2 , independent of β , such that for all $\beta \in \mathbb{R}^d$:

$$M_1 \cdot \pi_{\text{ALD}}(\beta | \theta, \mathbf{y}, \mathbf{X}; \tau) \leq \pi_{\text{BSQR}}(\beta | \theta, \mathbf{y}, \mathbf{X}; \tau, h) \leq M_2 \cdot \pi_{\text{ALD}}(\beta | \theta, \mathbf{y}, \mathbf{X}; \tau).$$

Remark 4. *Theorem 4* suggests that for BSQR models using compact support kernels, the overall shape and tail behavior of the posterior for β are similar to those of the standard ALD-based QR posterior. This provides theoretical justification for using BSQR as a computationally convenient alternative (e.g., for HMC sampling of β) without fundamentally altering the inferential conclusions regarding β , especially concerning tail properties. The equivalence holds up to a scaling factor, which is absorbed into the normalizing constants. This is distinct from BSQR with non-compact kernels (like Gaussian), where $L_h(e; \tau) - \rho_\tau(e)$ may not be bounded for all e , potentially leading to different tail behaviors.

5.2 Kernel effects on posterior concentration

Beyond the equivalence in tail behavior under compact support kernels, the specific choice of kernel $K(\cdot)$ can influence other characteristics of the BSQR posterior, notably its concentration around the mode. Intuitively, a kernel function that is more “peaked”—or assigns greater weight to residuals near zero (when scaled by h)—might lead to a smoothed loss component of the log-likelihood that penalizes deviations from zero more sharply. This, in turn, could result in a posterior distribution for β that is more concentrated. We formalize this intuition by examining the Hessian of the negative log-likelihood component of the posterior.

Let $U_L(\beta; \theta, h, K) = \theta \sum_{i=1}^n L_h(e_i(\beta); \tau)$ be the primary component of the negative log-posterior (or potential energy function) that depends on β through the sum of smoothed losses, with its argument K signifying dependence on the kernel function $K(\cdot)$. The full negative log-posterior is $U(\beta) = U_L(\beta; \theta, h, K) - \log \pi(\beta) + C_{\theta, h}$, where $C_{\theta, h}$ collects terms not dependent on β . The Hessian of $U(\beta)$ with respect to β is $\mathbf{H}(\beta) := \nabla_\beta^2 U(\beta) = \nabla_\beta^2 U_L(\beta; \theta, h, K) - \nabla_\beta^2 \log \pi(\beta)$.

To find the second derivative of $L_h(e; \tau)$, we differentiate the smoothed score function $\Psi_h(e; \tau)$ from Eq. (8) with respect to e :

$$\frac{\partial \Psi_h(e; \tau)}{\partial e} = \frac{\partial}{\partial e} ((\psi_\tau * K_h)(e)) = (\psi'_\tau * K_h)(e).$$

The derivative of $\psi_\tau(u) = \tau - \mathbb{I}(u < 0)$ is $\psi'_\tau(u) = \delta(u)$, where $\delta(u)$ is the Dirac delta function.⁵ Thus, we obtain

$$\frac{\partial \Psi_h(e; \tau)}{\partial e} = (\delta * K_h)(e) = \int_{-\infty}^{\infty} \delta(v) K_h(e - v) dv = K_h(e - 0) = \frac{1}{h} K\left(\frac{e}{h}\right),$$

⁵Strictly speaking, the classical derivative of $\psi_\tau(u)$ does not exist at $u = 0$ due to the discontinuity. However, in the distributional sense, it is given by $\psi'_\tau(u) = \delta(u)$. To see this, note that $\psi_\tau(u) = \tau - 1 + H(u)$, where $H(u)$ is the Heaviside step function ($H(u) = 0$ for $u < 0$ and $H(u) = 1$ for $u \geq 0$). The distributional derivative of $H(u)$ is the Dirac delta $\delta(u)$, leading to $\psi'_\tau(u) = \delta(u)$. This does not affect the convolution, which yields a smooth second derivative.

by utilizing the sifting property of the Dirac delta function, which states $\int_{-\infty}^{\infty} f(x)\delta(x-a) dx = f(a)$.

We now derive the Hessian of $U_L(\beta; \theta, h, K)$, denoted as $\mathbf{H}_L(\beta; K)$. The first gradient of $U_L(\beta; \theta, h, K)$ with respect to β is:

$$\nabla_{\beta} U_L(\beta; \theta, h, K) = \theta \sum_{i=1}^n \frac{\partial L_h(e_i(\beta); \tau)}{\partial \beta} = \theta \sum_{i=1}^n \left(\frac{\partial L_h(e_i; \tau)}{\partial e_i} \cdot \frac{\partial e_i(\beta)}{\partial \beta} \right) = \theta \sum_{i=1}^n \Psi_h(e_i(\beta); \tau)(-\mathbf{x}_i),$$

since $\partial e_i / \partial \beta = -\mathbf{x}_i$. The Hessian is obtained by differentiating the gradient with respect to β^\top :

$$\begin{aligned} \mathbf{H}_L(\beta; K) &= \nabla_{\beta^\top} \left(-\theta \sum_{i=1}^n \Psi_h(e_i(\beta); \tau) \mathbf{x}_i \right) = -\theta \sum_{i=1}^n \frac{\partial}{\partial \beta^\top} (\Psi_h(e_i(\beta); \tau) \mathbf{x}_i) \\ &= -\theta \sum_{i=1}^n \mathbf{x}_i \frac{\partial \Psi_h(e_i(\beta); \tau)}{\partial \beta^\top} = -\theta \sum_{i=1}^n \mathbf{x}_i \left(\frac{\partial \Psi_h(e_i; \tau)}{\partial e_i} \cdot \frac{\partial e_i(\beta)}{\partial \beta^\top} \right) \\ &= -\theta \sum_{i=1}^n \mathbf{x}_i \left(\frac{1}{h} K \left(\frac{e_i(\beta)}{h} \right) \cdot (-\mathbf{x}_i^\top) \right) = \frac{\theta}{h} \sum_{i=1}^n K \left(\frac{e_i(\beta)}{h} \right) \mathbf{x}_i \mathbf{x}_i^\top. \end{aligned} \quad (16)$$

A larger Hessian (in the positive definite sense) at the posterior mode $\check{\beta}$ suggests a more sharply peaked posterior and, via Laplace approximation, a smaller posterior covariance.

As discussed in Section 3, the true errors $\varepsilon_{0i} = y_i - \mathbf{x}_i^\top \beta_0(\tau)$ are assumed to be independent and identically distributed following a common density $f_{\varepsilon_0}(\cdot)$, where $\beta_0(\tau)$ represents the true value of $\beta(\tau)$. Define $s_K(h) := \mathbb{E}_{\varepsilon_0 \sim f_{\varepsilon_0}} [K(\frac{\varepsilon_0}{h})]$. Let $\mathcal{H}_L(\beta_0(\tau); K) := \mathbb{E}_{\varepsilon_{0i}, \mathbf{x}_i} [\mathbf{H}_L(\beta_0(\tau); K)]$ denote the expected Hessian of the negative log-likelihood component, evaluated at the true parameter $\beta_0(\tau)$. This leads to the following theorem with the proof provided in [Appendix A](#).

Theorem 5 (Kernel peakedness and expected local curvature). *Let $K_A(v)$ and $K_B(v)$ be two distinct kernel functions that are non-negative, symmetric about zero, and share a common compact support. Assume that $s_{K_A}(h) > s_{K_B}(h)$, and that the covariates follow $\mathbf{x}_i \stackrel{i.i.d.}{\sim} P_{\mathbf{X}}$ where $P_{\mathbf{X}}$ has a positive definite covariance matrix $\Sigma_x := \mathbb{E}[\mathbf{x}_i \mathbf{x}_i^\top]$ and finite second moments. Then, for the expected Hessian:*

$$\mathcal{H}_L(\beta_0(\tau); K_A) > \mathcal{H}_L(\beta_0(\tau); K_B),$$

where $>$ denotes the strict Loewner order. Furthermore, for the sample Hessian, the corresponding inequality

$$\mathbf{H}_L(\beta_0(\tau); K_A) > \mathbf{H}_L(\beta_0(\tau); K_B)$$

holds with probability approaching 1 as $n \rightarrow \infty$.

Remark 5. *Theorem 5 establishes that if the condition $s_{K_A}(h) > s_{K_B}(h)$ holds, the kernel K_A leads to a larger expected Hessian of the negative log-likelihood component at the true parameter $\beta_0(\tau)$ compared to K_B . This increased local curvature, via Laplace approximation, suggests a more concentrated posterior distribution for β under kernel K_A . Consequently, this implies a potentially smaller posterior covariance matrix (i.e., $\mathcal{H}_L(\beta_0(\tau); K_A)^{-1} \leq \mathcal{H}_L(\beta_0(\tau); K_B)^{-1}$), assuming the contribution from the prior's Hessian is negligible or identical for both kernels.*

Remark 6. The key condition $s_{K_A}(h) > s_{K_B}(h)$ signifies that kernel K_A assigns, on average, more weight to the true scaled errors ε_0/h than kernel K_B . This inequality is intuitively more likely to be satisfied if $K_A(v)$ is more “peaked” or concentrated around $v = 0$ relative to $K_B(v)$, particularly when the true error density $f_{\varepsilon_0}(\cdot)$ is also concentrated around 0, leading to ε_0/h values frequently occurring near 0. For instance, comparing a Triangular kernel ($K_T(0) = 1$) with a Uniform kernel ($K_U(0) = 0.5$) on $[-1, 1]$, if $f_{\varepsilon_0}(\cdot)$ and h are such that most ε_0/h values fall within an interval like $[-0.5, 0.5]$ where $K_T(v)$ exceeds $K_U(v)$, the condition might hold.

Remark 7. While [Theorem 5](#) focuses on the expected behavior at the true parameter $\beta_0(\tau)$, its underlying principle regarding kernel shape and curvature can be informative for understanding behavior at a posterior mode $\check{\beta}$. Similar arguments about posterior concentration might apply locally if the empirical distribution of the scaled residuals $e_i(\check{\beta})/h$ results in a consistent ordering of the sums $\sum_{i=1}^n K(e_i(\check{\beta})/h)$ when comparing different kernels.

6 Bayesian inference via MCMC

Estimating the parameters of the BSQR model and quantifying their uncertainty presents an inferential challenge. This section details a comprehensive Bayesian approach designed to address this, focusing on the regression coefficients β and an additional positive scale parameter θ . Directly sampling from this joint posterior distribution is often intractable. Standard BQR frequently capitalizes on the representation of the ALD as a scale mixture of normals, facilitating efficient Gibbs sampling schemes ([Yu & Moyeed, 2001](#); [Kozumi & Kobayashi, 2011](#)). However, the introduction of the smoothed loss $L_h(e; \tau)$ in the BSQR framework, while beneficial for gradient-based optimization and theoretical properties, typically disrupts the conditional conjugacy required for such straightforward Gibbs updates.

To surmount this obstacle, we engineer a bespoke hybrid MCMC algorithm. This strategy involves iteratively drawing samples from the full conditional posterior distributions. Specifically, the high-dimensional regression coefficient vector β is updated using HMC, an advanced gradient-informed sampler particularly adept at navigating complex, high-dimensional target densities ([Duane et al., 1987](#); [Neal, 2011](#)); this procedure is elaborated in Section 6.1. Complementing this, the scalar parameter θ is updated using a Metropolis-Hastings (MH) step ([Metropolis et al., 1953](#); [Hastings, 1970](#)), which is well-suited for target densities where normalizing constants depend on the parameter being sampled, as detailed in Section 6.2. This carefully constructed block-wise MCMC approach enables robust and efficient exploration of the intricate posterior landscape of the BSQR model.

6.1 Hamiltonian Monte Carlo sampling for β

We have adopted a Bayesian framework to perform inference on the parameters β and an additional precision parameter $\theta > 0$ within the SQR model. While Gibbs sampling offers an efficient strategy for standard Bayesian quantile regression due to the ALD's representation as a scale mixture of normals (Yu & Moyeed, 2001; Kozumi & Kobayashi, 2011), this is generally not applicable to the BSQR model. The convolution in $L_h(e; \tau)$ typically disrupts the conditional conjugacy needed for full Gibbs updates.

Consequently, we employ a hybrid MCMC approach. To sample from the conditional posterior $\pi(\beta | \theta_c, \mathbf{y}, \mathbf{X}; \tau, h)$, where θ_c denotes the current (fixed) value of θ (e.g., from the previous iteration or initial value), we employ HMC (Duane et al., 1987; Neal, 2011). The parameter θ will subsequently be updated conditional on the newly sampled β , using an MH step as detailed in Section 6.2. HMC is an advanced MCMC method that avoids the random walk behavior of simpler algorithms by introducing auxiliary momentum variables and simulating Hamiltonian dynamics. This allows for efficient exploration of complex, high-dimensional parameter spaces, particularly when gradients of the target density are available, as is the case for the BSQR likelihood conditional on θ_c .

In the HMC framework applied to β , we augment the d -dimensional parameter vector β with an auxiliary d -dimensional momentum vector \mathbf{p} . The system's dynamics are governed by the Hamiltonian function $H(\beta, \mathbf{p})$, representing the total energy:

$$H(\beta, \mathbf{p}) = U(\beta | \theta_c, \mathbf{y}, \mathbf{X}) + T(\mathbf{p}).$$

The potential energy $U(\beta | \theta_c, \mathbf{y}, \mathbf{X})$ is defined as the negative logarithm of the target conditional posterior density for β (ignoring terms constant with respect to β), given the current value of θ_c :

$$U(\beta | \theta_c, \mathbf{y}, \mathbf{X}) = \theta_c \sum_{i=1}^n L_h(e_i(\beta); \tau) - \log \pi(\beta). \quad (17)$$

The kinetic energy $T(\mathbf{p})$ is typically a quadratic function of the momentum:

$$T(\mathbf{p}) = \frac{1}{2} \mathbf{p}^\top \mathbf{M}^{-1} \mathbf{p},$$

where \mathbf{M} is a symmetric positive-definite mass matrix, often taken as the identity matrix \mathbf{I} . The evolution of $(\beta(s), \mathbf{p}(s))$ over a fictitious time s is described by Hamilton's equations (Duane et al., 1987; Neal, 2011):

$$\begin{aligned} \frac{d\beta(s)}{ds} &= \frac{\partial H}{\partial \mathbf{p}(s)} = \mathbf{M}^{-1} \mathbf{p}(s), \\ \frac{d\mathbf{p}(s)}{ds} &= -\frac{\partial H}{\partial \beta(s)} = -\nabla_\beta U(\beta(s) | \theta, \mathbf{y}, \mathbf{X}). \end{aligned}$$

HMC numerically integrates these equations using the leapfrog method. Given current values β and \mathbf{p} , a single leapfrog step of size ϵ updates them to β' and \mathbf{p}' as follows:

$$\mathbf{p}_{\text{half}} = \mathbf{p} - \frac{\epsilon}{2} \nabla_\beta U(\beta | \theta, \mathbf{y}, \mathbf{X}),$$

$$\begin{aligned}\boldsymbol{\beta}' &= \boldsymbol{\beta} + \epsilon \mathbf{M}^{-1} \mathbf{p}_{\text{half}}, \\ \mathbf{p}' &= \mathbf{p}_{\text{half}} - \frac{\epsilon}{2} \nabla_{\boldsymbol{\beta}} U(\boldsymbol{\beta}' \mid \theta, \mathbf{y}, \mathbf{X}).\end{aligned}$$

The HMC algorithm for generating N samples of $\boldsymbol{\beta}$ given a fixed θ_c (and other model constants) is detailed in [Algorithm 1](#) of [Appendix B](#).

The critical component for the leapfrog integrator is the gradient of the potential energy, $\nabla_{\boldsymbol{\beta}} U(\boldsymbol{\beta} \mid \theta, \mathbf{y}, \mathbf{X})$. From Eq. (17), we derive that

$$\nabla_{\boldsymbol{\beta}} U(\boldsymbol{\beta} \mid \theta, \mathbf{y}, \mathbf{X}) = \theta \sum_{i=1}^n \nabla_{\boldsymbol{\beta}} L_h(e_i(\boldsymbol{\beta}); \tau) - \nabla_{\boldsymbol{\beta}} \log \pi(\boldsymbol{\beta}).$$

Recalling that $\Psi_h(e; \tau) = \int_{-\infty}^{\infty} \psi_{\tau}(u) K_h(e-u) du$ in Eq. (8), we substitute the definitions of $\psi_{\tau}(u)$ and $K_h(e-u)$, and obtain

$$\begin{aligned}\Psi_h(e; \tau) &= \int_{-\infty}^{\infty} (\tau - \mathbb{I}(u < 0)) \frac{1}{h} K\left(\frac{e-u}{h}\right) du \\ &= \tau \int_{-\infty}^{\infty} \frac{1}{h} K\left(\frac{e-u}{h}\right) du - \int_{-\infty}^{\infty} \mathbb{I}(u < 0) \frac{1}{h} K\left(\frac{e-u}{h}\right) du \\ &= \tau \int_{\infty}^{-\infty} K(z) (-dz) - \int_{-\infty}^0 \frac{1}{h} K\left(\frac{e-u}{h}\right) du \\ &= \tau \int_{-\infty}^{\infty} K(z) dz - \int_{e/h}^{\infty} K(z) dz \\ &= \tau - \left(1 - \int_{-\infty}^{e/h} K(z) dz\right) \\ &= \tau - \left(1 - F_K\left(\frac{e}{h}\right)\right) = F_K\left(\frac{e}{h}\right) - (1 - \tau),\end{aligned}\tag{18}$$

where $F_K(x) = \int_{-\infty}^x K(s) ds$ represents the CDF of the standard kernel $K(\cdot)$. Assuming a Gaussian prior $\boldsymbol{\beta} \sim \mathcal{N}(\boldsymbol{\beta}_0, \Omega)$, for which $\nabla_{\boldsymbol{\beta}} \log \pi(\boldsymbol{\beta}) = -\Omega^{-1}(\boldsymbol{\beta} - \boldsymbol{\beta}_0)$, the complete gradient of the potential energy is:

$$\nabla_{\boldsymbol{\beta}} U(\boldsymbol{\beta} \mid \theta, \mathbf{y}, \mathbf{X}) = -\theta \sum_{i=1}^n \left[F_K\left(\frac{e_i(\boldsymbol{\beta})}{h}\right) - (1 - \tau) \right] \mathbf{x}_i + \Omega^{-1}(\boldsymbol{\beta} - \boldsymbol{\beta}_0).$$

The evaluation of $U(\boldsymbol{\beta} \mid \theta, \mathbf{y}, \mathbf{X})$ in the acceptance step (Eq. (B.1)) necessitates the specific form of $L_h(e_i; \tau)$ corresponding to the chosen kernel. The expressions for $\Psi_h(e; \tau)$ and the derivation of $L_h(e; \tau)$ for several common standard kernels $K(v)$ are detailed below. The detailed derivations are provided in [Appendix C](#).

6.1.1 Gaussian kernel

The standard Gaussian kernel is $K(v) = \phi(v) = (2\pi)^{-1/2} \exp(-v^2/2)$, with CDF $F_K(u) = \Phi(u)$. Applying Eq. (18) yields:

$$\Psi_h(e; \tau) = \Phi\left(\frac{e}{h}\right) - (1 - \tau).\tag{19}$$

The corresponding smoothed loss function $L_h(e; \tau)$, obtained by integrating $\Psi_h(e; \tau)$ and consistent with $\rho_\tau(e)$ for small h , is given by (e.g., [Horowitz, 1998](#); [Koenker, 2005](#)):

$$L_h(e; \tau) = e \left(\Phi \left(\frac{e}{h} \right) - (1 - \tau) \right) + h \phi \left(\frac{e}{h} \right).$$

6.1.2 Uniform kernel

The standard Uniform kernel is $K(v) = \frac{1}{2}$ for $v \in [-1, 1]$ and 0 otherwise. Its CDF is $F_K(u) = 0$ for $u < -1$, $F_K(u) = \frac{u+1}{2}$ for $-1 \leq u \leq 1$, and $F_K(u) = 1$ for $u > 1$. From Eq. (18), $\Psi_h(e; \tau)$ is:

$$\Psi_h(e; \tau) = \begin{cases} -(1 - \tau) & \text{if } e/h < -1, \\ \frac{e}{2h} + \tau - \frac{1}{2} & \text{if } -1 \leq e/h \leq 1, \\ \tau & \text{if } e/h > 1. \end{cases}$$

The function $L_h(e; \tau)$ is derived by integrating $\Psi_h(e; \tau)$ and imposing continuity with $\rho_\tau(e)$ for $|e/h| \geq 1$. The resulting expression is:

$$L_h(e; \tau) = \begin{cases} e(\tau - 1) & \text{if } e/h \leq -1, \\ \frac{e^2}{4h} + e \left(\tau - \frac{1}{2} \right) + \frac{h}{4} & \text{if } -1 < e/h < 1, \\ e\tau & \text{if } e/h \geq 1. \end{cases}$$

6.1.3 Epanechnikov kernel

The standard Epanechnikov kernel is $K(v) = \frac{3}{4}(1 - v^2)$ for $v \in [-1, 1]$ and 0 otherwise. Its CDF, $F_K(u)$, is 0 for $u < -1$, $\frac{3}{4}u - \frac{1}{4}u^3 + \frac{1}{2}$ for $-1 \leq u \leq 1$, and 1 for $u > 1$. This yields $\Psi_h(e; \tau)$ as:

$$\Psi_h(e; \tau) = \begin{cases} -(1 - \tau) & \text{if } e/h < -1, \\ \frac{3}{4} \frac{e}{h} - \frac{1}{4} \left(\frac{e}{h} \right)^3 + \tau - \frac{1}{2} & \text{if } -1 \leq e/h \leq 1, \\ \tau & \text{if } e/h > 1. \end{cases}$$

Integration of $\Psi_h(e; \tau)$ and matching boundary conditions with $\rho_\tau(e)$ for $|e/h| \geq 1$ leads to $L_h(e; \tau)$:

$$L_h(e; \tau) = \begin{cases} e(\tau - 1) & \text{if } e/h \leq -1, \\ \frac{3e^2}{8h} - \frac{e^4}{16h^3} + e \left(\tau - \frac{1}{2} \right) + \frac{3h}{16} & \text{if } -1 < e/h < 1, \\ e\tau & \text{if } e/h \geq 1. \end{cases}$$

6.1.4 Triangular kernel

The standard Triangular kernel is $K(v) = 1 - |v|$ for $v \in [-1, 1]$ and 0 otherwise. The CDF, $F_K(u)$, is 0 for $u < -1$; $\frac{1}{2}(1 + u)^2$ for $-1 \leq u < 0$; $1 - \frac{1}{2}(1 - u)^2$ for $0 \leq u \leq 1$; and 1 for $u > 1$. Consequently,

$\Psi_h(e; \tau)$ is:

$$\Psi_h(e; \tau) = \begin{cases} -(1 - \tau) & \text{if } e/h < -1, \\ \frac{1}{2} \left(1 + \frac{e}{h}\right)^2 - (1 - \tau) & \text{if } -1 \leq e/h < 0, \\ 1 - \frac{1}{2} \left(1 - \frac{e}{h}\right)^2 - (1 - \tau) & \text{if } 0 \leq e/h \leq 1, \\ \tau & \text{if } e/h > 1. \end{cases}$$

The corresponding $L_h(e; \tau)$ is obtained by piecewise integration of $\Psi_h(e; \tau)$, ensuring continuity with $\rho_\tau(e)$ for $|e/h| \geq 1$ and at $e = 0$:

$$L_h(e; \tau) = \begin{cases} e(\tau - 1) & \text{if } e/h \leq -1, \\ \frac{h}{6} \left(1 + \frac{e}{h}\right)^3 - e(1 - \tau) & \text{if } -1 < e/h < 0, \\ e\tau + \frac{h}{6} \left(1 - \frac{e}{h}\right)^3 & \text{if } 0 \leq e/h < 1, \\ e\tau & \text{if } e/h \geq 1. \end{cases}$$

The computational cost of HMC is primarily driven by the J gradient evaluations per MCMC iteration. The leapfrog step size ϵ and number of steps J are crucial tuning parameters, often managed adaptively using methods like the NUTS (Hoffman & Gelman, 2014), as implemented in software such as Stan (Carpenter et al., 2017) and PyMC (Salvatier et al., 2016). The mass matrix M can also be adapted. The HMC algorithm detailed in [Algorithm 1](#) describes how to sample β from its conditional posterior $\pi(\beta | \theta_c, \mathbf{y}, \mathcal{X})$, treating the current value of the parameter θ (denoted as θ_c within [Algorithm 1](#)) as fixed for this specific update. In the broader MCMC framework for inferring both β and θ from their joint posterior $\pi(\beta, \theta | \mathbf{y}, \mathcal{X})$, this HMC step for β is alternated with a step to update θ conditional on the most recent sample of β (as detailed in [Section 6.2](#)). Applying HMC jointly to (β, θ) is complicated by the intractability of $\partial \log Z(\theta, \tau, h) / \partial \theta$, which motivates this hybrid MCMC approach where different samplers are used for β and θ .

6.2 Metropolis-Hastings sampling for θ

Following the HMC-based sampling of the regression coefficients β conditional on the precision parameter θ , we now address the inference for θ itself. The full Bayesian model requires that θ also be sampled from its conditional posterior distribution, $\pi(\theta | \beta_c, \mathbf{y}, \mathcal{X}; \tau, h)$, where β_c denotes the current (most recently sampled) value of β from [Section 6.1](#). While HMC has been proved to be effective for the high-dimensional β vector, its application to θ presents significant challenges. The primary difficulty arises from the normalizing constant $Z(\theta, \tau, h)$ defined in [Eq. \(11\)](#). The potential energy for θ would involve terms like $n \log Z(\theta, \tau, h)$. Calculating the gradient of this term with respect to θ for HMC, i.e., $\frac{\partial}{\partial \theta} \log Z(\theta, \tau, h)$, requires differentiating $Z(\theta, \tau, h)$, which involves an integral of the

form $\int_{-\infty}^{\infty} -L_h(u; \tau) \exp(-\theta L_h(u; \tau)) du$. Both $Z(\theta, \tau, h)$ and its derivative typically lack closed-form expressions and would necessitate computationally intensive numerical integration within each leapfrog step of an HMC trajectory.

Consequently, we opt for an MH algorithm to sample θ . The MH algorithm only requires evaluation of the target posterior density rather than its gradient. The target conditional posterior for θ is:

$$\pi(\theta | \beta_c, \mathbf{y}, \mathbf{X}) \propto \left(\prod_{i=1}^n \frac{1}{Z(\theta, \tau, h)} \exp(-\theta L_h(e_i(\beta_c); \tau)) \right) \pi(\theta),$$

which can be rewritten as:

$$\pi(\theta | \beta_c, \mathbf{y}, \mathbf{X}) \propto Z(\theta, \tau, h)^{-n} \exp \left(-\theta \sum_{i=1}^n L_h(e_i(\beta_c); \tau) \right) \pi(\theta).$$

In physics and certain statistical models, the probability distribution $\pi(\cdot)$ can often be expressed as $\pi(\cdot) \propto \exp(-U(\cdot))$, where $U(\cdot)$ is termed the *potential energy function*. We define the potential energy function for θ ignoring terms constant with respect to θ as:

$$U_\theta(\theta | \beta_c, \mathbf{y}, \mathbf{X}) = -\log \pi(\theta | \beta_c, \mathbf{y}, \mathbf{X}) = \theta \sum_{i=1}^n L_h(e_i(\beta_c); \tau) + n \log Z(\theta, \tau, h) - \log \pi(\theta) + C, \quad (20)$$

where C is a constant independent of θ . We typically assume a Gamma prior for the precision parameter $\theta \sim \text{Gamma}(a_\theta, b_\theta)$.

A common choice for the proposal distribution $q(\theta' | \theta_c)$ for a positive parameter like θ' is a log-normal proposal: $\log \theta' \sim \mathcal{N}(\log \theta_c, \sigma_{\log \theta}^2)$, where $\sigma_{\log \theta}^2$ is a tuning parameter. The PDF of $q(\theta' | \theta_c)$ is thus given by:

$$q(\theta' | \theta_c) = \frac{1}{\theta' \sigma_{\log \theta} \sqrt{2\pi}} \exp \left(-\frac{(\log \theta' - \log \theta_c)^2}{2\sigma_{\log \theta}^2} \right).$$

Similarly, for the reverse proposal $q(\theta_c | \theta')$, we consider proposing θ_c from θ' . The underlying mechanism implies that $\log \theta_c \sim \mathcal{N}(\log \theta', \sigma_{\log \theta}^2)$. Therefore, the PDF of $q(\theta_c | \theta')$ is:

$$q(\theta_c | \theta') = \frac{1}{\theta_c \sigma_{\log \theta} \sqrt{2\pi}} \exp \left(-\frac{(\log \theta_c - \log \theta')^2}{2\sigma_{\log \theta}^2} \right).$$

The Hastings ratio is then calculated as the ratio of these two densities:

$$\frac{q(\theta_c | \theta')}{q(\theta' | \theta_c)} = \frac{\frac{1}{\theta_c \sigma_{\log \theta} \sqrt{2\pi}} \exp \left(-\frac{(\log \theta_c - \log \theta')^2}{2\sigma_{\log \theta}^2} \right)}{\frac{1}{\theta' \sigma_{\log \theta} \sqrt{2\pi}} \exp \left(-\frac{(\log \theta' - \log \theta_c)^2}{2\sigma_{\log \theta}^2} \right)} = \frac{1/\theta_c}{1/\theta'} = \frac{\theta'}{\theta_c}. \quad (21)$$

Moreover, the log acceptance ratio, $\log r$, proposing θ^* from the current value θ_c is:

$$\log r = \log \pi(\theta^* | \beta_c, \mathbf{y}, \mathbf{X}) - \log \pi(\theta_c | \beta_c, \mathbf{y}, \mathbf{X}) + \log \left(\frac{q(\theta_c | \theta^*)}{q(\theta^* | \theta_c)} \right).$$

Using the potential energy $U_\theta(\theta | \beta_c, \mathbf{y}, \mathbf{X}) = -\log \pi(\theta | \beta_c, \mathbf{y}, \mathbf{X})$ (defined in Eq. (20)) and Eq. (21), we have:

$$\log r = U_\theta(\theta_c | \beta, \mathbf{y}, \mathbf{X}) - U_\theta(\theta^* | \beta, \mathbf{y}, \mathbf{X}) + (\log \theta^* - \log \theta_c). \quad (22)$$

From Eq. (20) and the Gamma prior $\log \pi(\theta) = (a_\theta - 1) \log \theta - b_\theta \theta + \text{const.}$, $U_\theta(\theta | \beta, \mathbf{y}, \mathbf{X})$ becomes:

$$U_\theta(\theta | \beta, \mathbf{y}, \mathbf{X}) = \theta S(\beta_c; \tau, h) + n \log Z(\theta, \tau, h) - ((a_\theta - 1) \log \theta - b_\theta \theta)$$

by ignoring constants, where $S(\beta_c; \tau, h) = \sum_{i=1}^n L_h(e_i(\beta_c); \tau)$. Substituting this into Eq. (22), we finally get that

$$\begin{aligned} \log r &= [\theta_c S(\beta_c; \tau, h) + n \log Z(\theta_c, \tau, h) - ((a_\theta - 1) \log \theta_c - b_\theta \theta_c)] \\ &\quad - [\theta^* S(\beta_c; \tau, h) + n \log Z(\theta^*, \tau, h) - ((a_\theta - 1) \log \theta^* - b_\theta \theta^*)] + (\log \theta^* - \log \theta_c) \\ &= -(\theta^* - \theta_c) S(\beta_c; \tau, h) - n(\log Z(\theta^*, \tau, h) - \log Z(\theta_c, \tau, h)) \\ &\quad + a_\theta (\log \theta^* - \log \theta_c) - b_\theta (\theta^* - \theta_c). \end{aligned}$$

This expression for $\log r$ is utilized in the MH Algorithm. The specific forms of $L_h(e; \tau)$ for various kernels, as detailed in Sections 6.1.1 to 6.1.4, are used to compute $S(\beta_c; \tau, h)$ (which appears in $\log r$). The evaluation of $Z(\theta, \tau, h)$ generally requires numerical integration for these kernels. The MH algorithm for sampling θ is detailed in [Algorithm 2](#) of [Appendix B](#).

The critical step in [Algorithm 2](#) is the numerical evaluation of $Z(\theta, \tau, h)$. While computationally non-trivial, it is generally more manageable than evaluating its gradient as required by HMC. The overall MCMC procedure would then iterate between running [Algorithm 1](#) and running [Algorithm 2](#) to sample θ conditional on the newly sampled β . This iterative block sampling strategy (Metropolis-within-Gibbs) allows for inference from the joint posterior $\pi(\beta, \theta | \mathbf{y}, \mathbf{X}; \tau, h)$.

7 Simulation

In this section, we present a comprehensive simulation study to evaluate the performance of our proposed BSQR framework. We assess the estimation accuracy and inferential validity of BSQR using different kernel functions (Gaussian, Uniform, Epanechnikov, and Triangular, as discussed in Sections 6.1.1 to 6.1.4) and compare it to established frequentist and Bayesian quantile regression methods. The R and Stan code to replicate all results presented in this section is provided in the `Simulation/` directory of the public repository mentioned in the introduction.

Synthetic datasets are generated from the linear model $y_i = \mathbf{x}_i^\top \beta_0 + u_i$ for $i = 1, \dots, n$. For each replication, we generate a training set of size $N_{\text{train}} = 200$ and a separate test set of size $N_{\text{test}} = 1000$. The d -dimensional covariate vectors \mathbf{x}_i follow a multivariate normal distribution, $\mathbf{x}_i \sim \mathcal{N}(\mathbf{0}, \Sigma_X)$,

where the covariance matrix Σ_X has an autoregressive structure $(\Sigma_X)_{jk} = \rho^{|j-k|}$ with $\rho = 0.5$, as in [Fan and Li \(2001\)](#). We consider two scenarios for the true coefficients: a sparse, high-dimensional setting ($d = 20$) with $\beta_0 = (3, 1.5, 0, 0, 2, 0, \dots, 0)^\top$, and a dense, lower-dimensional setting ($d = 8$) with $\beta_0 = (0.85, 0.85, \dots, 0.85)^\top$. To evaluate robustness, we employ four error distributions for u_i : (1) standard normal, $u_i \sim \mathcal{N}(0, 1)$; (2) heavy-tailed Student's t , $u_i \sim t(3)$; (3) bimodal mixture normal, $u_i \sim 0.2\mathcal{N}(0, 3) + 0.8\mathcal{N}(0, 4)$; and (4) heteroscedastic normal, $u_i \mid \mathbf{x}_i \sim \mathcal{N}(0, \sigma_i^2)$ with $\sigma_i = \exp(-0.25 + 0.5x_{i1})$.⁶ Simulations are conducted for quantile levels $\tau \in \{0.25, 0.5, 0.75\}$, with $M = 200$ independent replications per setting.

Benchmark methods include classical frequentist standard quantile regression (StdQR), implemented via the “rq” function in the `quantreg` package in R, and Bayesian quantile regression based on the asymmetric Laplace distribution (BQR-ALD), implemented using the `brms` package. BSQR methods are implemented in Stan, employing the No-U-Turn sampler (NUTS) ([Hoffman & Gelman, 2014](#)) for joint posterior inference. Computations are parallelized; for each replication, we run two MCMC chains of 4000 iterations each, discarding the first 2000 as warm-up, yielding 4000 post-warm-up samples without thinning.

A key computational element in BSQR is the evaluation of the normalizing constant $Z(\theta, \tau, h)$ in the kernel-smoothed likelihood. This constant, depending on θ , τ , and h , is computed at each NUTS step. To ensure efficiency and accuracy, we use a hybrid approach: an asymptotic approximation for sharply peaked integrands (e.g., large θ or specific τ and h), avoiding instability and reducing time; otherwise, direct numerical integration via Stan’s “`integrate_1d`” function.

For all Bayesian methods, we adopt weakly informative priors: $\beta \sim \mathcal{N}(\mathbf{0}, 1000\mathbf{I})$ and $\theta \sim \text{Gamma}(0.01, 0.01)$. Bandwidth h in BSQR is selected via 5-fold cross-validation on a grid (0.5, 0.75, 1.0, 1.5, and 2.0 times Silverman’s rule), minimizing average check loss.

Performance is assessed using a suite of evaluation metrics. The values reported in our results are the averages over the $M = 200$ replications, serving as Monte Carlo estimates of the metrics’ theoretical expectations. For a single replication, these metrics are defined as follows. Point estimation accuracy is measured by the mean squared error (MSE), $\|\hat{\beta} - \beta_0\|_2^2$; the mean absolute error (MAE), $\|\hat{\beta} - \beta_0\|_1/d$; and the weighted mean squared error (WMSE), $(\hat{\beta} - \beta_0)^\top \Sigma_X (\hat{\beta} - \beta_0)$, where $\hat{\beta}$ is the posterior mean. Out-of-sample predictive performance is evaluated on the independent test set using the average check loss, $1/N_{\text{test}} \sum_{i=1}^{N_{\text{test}}} \rho_\tau(y_i^{\text{test}} - \mathbf{x}_i^{\text{test}} \hat{\beta})$. For Bayesian methods, we also report the empirical coverage and average width of 95% credible intervals, computation time (seconds), and MCMC diagnostics, including the maximum potential scale reduction factor (\hat{R}_{\max}) and the minimum bulk effective sample size (ESS_{\min})

⁶Note that error settings (1)–(3) correspond to a homoscedastic location-shift model, which satisfies the linear conditional quantile assumption. Setting (4) introduces heteroscedasticity where the conditional quantile function is no longer linear in covariates. This allows us to evaluate the robustness of our BSQR framework under this form of model misspecification.

across all β coefficients. Simulation results are detailed in Table D of Appendix D.

The simulation results validate the proposed BSQR framework, showing consistent superiority over standard BQR-ALD across multiple dimensions. BSQR generally excels in estimation accuracy and prediction, with lower MSE, MAE, and WMSE for coefficient estimates in most scenarios across error distributions, though BQR-ALD occasionally performs comparably or slightly better in specific cases. Critically, it resolves BQR-ALD's predictive bias: out-of-sample check loss is drastically reduced, matching the frequentist StdQR benchmark. At extreme quantile levels ($\tau = 0.25, 0.75$), BSQR achieves 40-50% lower loss; at the median ($\tau = 0.50$), performances are comparable. This confirms smoothing restores the link between parameters and true conditional quantiles. For inference, BSQR yields more reliable uncertainty quantification, with credible interval coverage often closer to 0.95. BQR-ALD's narrower intervals frequently under-cover, while BSQR provides honest estimates, especially with Uniform and Triangular kernels balancing coverage and width.

Computationally, BSQR's smoothed posterior enables efficient MCMC, with 20–40% higher minimum bulk ESS (e.g., 2700–3200 vs. 2100–2400 for BQR-ALD), ensuring reliable estimates. Bounded-support kernels (Uniform, Triangular, Epanechnikov) enhance stability (near-zero divergent transitions, consistently below 2), and Uniform is fastest, often surpassing BQR-ALD. Kernel comparisons highlight Uniform (BSQR-U) and Triangular (BSQR-T) as top choices: BSQR-U leads in speed for large data, while BSQR-T balances accuracy, speed, and inference. Epanechnikov (BSQR-E) is slower with wider intervals, dominated by Triangular; Gaussian (BSQR-G) is computationally intensive and least stable.

Overall, BSQR enhances Bayesian quantile regression by solving bias, improving efficiency, and favoring simple bounded-support *Uniform and Triangular kernels* for optimal trade-offs in speed, accuracy, and inference. These results endorse BSQR with uniform or triangular kernels for applied research.

8 Empirical analysis: Asymmetric systemic risk exposure in the post-COVID era

To demonstrate the empirical utility of our proposed BSQR framework, we investigate the asymmetric nature of dynamic systemic risk for a globally systemically important financial institution (G-SIFI). This section details the empirical methodology and results, highlighting BSQR's advantages in delivering more reliable risk quantification. As with the simulations, the code and data used for this empirical analysis are available in the `Empirical analysis/` directory of our public repository.

Our analysis models the relationship between the daily stock returns of JPMorgan Chase & Co. (JPM) and the S&P 500 Index (^GSPC)⁷. The data, comprising daily log-returns from January 1, 2017, to

⁷Data for JPM and the S&P 500 can be retrieved from <https://finance.yahoo.com/quote/JPM/> and <https://finance.yahoo.com/quote/^GSPC/>

January 1, 2025, were sourced from Yahoo Finance. After converting prices to continuously compounded returns ($r_t = \ln(P_t/P_{t-1})$), we obtain a rich time series whose summary statistics are presented in Table 1. The significant leptokurtosis observed in both series provides strong empirical motivation for a quantile-based approach.

Table 1. Descriptive statistics for daily log-returns.

Statistic	JPMorgan Chase (JPM)	S&P 500 Index (GSPC)
Observations	2011.0000	2011.0000
Mean	0.0006	0.0005
Std. Dev.	0.0178	0.0118
Skewness	-0.0240	-0.8614
Kurtosis	14.3309	16.2964

We specify a dynamic capital asset pricing model (CAPM) for a given quantile level τ :

$$Q_{\text{JPM_Return}_t}(\tau | \text{GSPC_Return}_t) = \alpha(\tau) + \beta(\tau) \cdot \text{GSPC_Return}_t.$$

The coefficient $\beta(\tau)$ measures systemic risk. To capture risk asymmetry, we focus on the downside beta ($\beta(0.05)$), quantifying exposure during severe market downturns, and the upside beta ($\beta(0.95)$), measuring participation in market rallies. We employ a rolling-window estimation with a one-year window (252 trading days), advanced by one month (21 trading days) per step, to compare our BSQR framework (Uniform and Triangular kernels) against the BQR-ALD benchmark across three dimensions: inferential stability and economic insight, predictive accuracy, and sampler efficiency.

8.1 Inferential stability and economic insights from asymmetric betas

The evolution of the dynamic betas, depicted in Figure 1, reveals two key findings. Methodologically, the BSQR framework yields substantially more stable and interpretable parameter estimates. In both panels, the credible intervals for the BQR-ALD benchmark (light gray shaded area) are visibly wider and more erratic than those produced by the BSQR models (orange and blue shaded areas). The BQR-ALD estimates are plagued by high-frequency noise, which can lead to over-interpretation of statistically insignificant fluctuations. In contrast, the kernel smoothing inherent in BSQR attenuates this noise, yielding tighter credible intervals and smoother posterior mean paths. This represents a more reliable quantification of uncertainty, enabling a clearer distinction between genuine shifts in the risk profile and mere sampling variation.

finance.yahoo.com/quote/^GSPC/, respectively.

Table 2. Out-of-sample forecasting performance for downside and upside quantile levels.

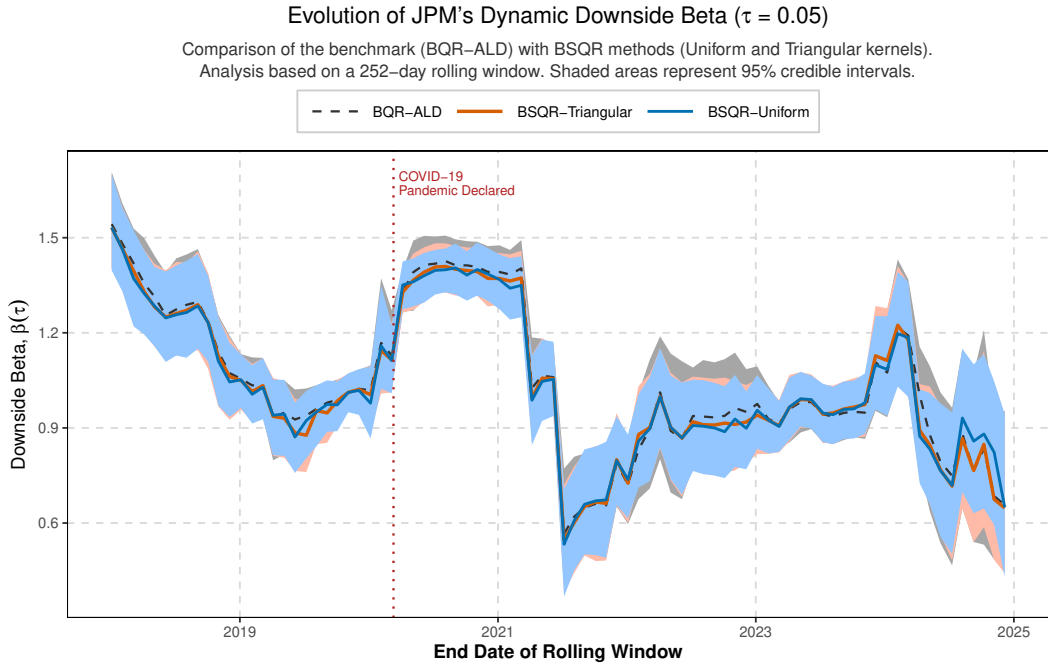
Methods	Downside ($\tau = 0.05$)	Upside ($\tau = 0.95$)
BQR-ALD	0.003027	0.001363
BSQR-Triangular	0.003031	0.001349
BSQR-Uniform	0.002998	0.001338

Economically, the inferential clarity of BSQR reveals a multi-phase and profoundly asymmetric response of JPM’s systemic risk to the COVID-19 shock. The initial market panic in early 2020 triggered a brief, sharp spike in both betas, visible as a symmetric upward jump in Figure 1. However, this transient reaction was quickly overshadowed by a more dominant and divergent dynamic over the subsequent months. The path of the downside beta ($\beta(0.05)$), which had been stable around a pre-crisis baseline averaging approximately 0.97, began a prolonged decoupling from market downturns. It plummeted to a visible trough of 0.53 by mid-2021, suggesting a sustained “flight-to-quality” effect. This de-risking behavior became a persistent feature, with the beta settling into a new, lower regime that averaged approximately 0.92 in the post-crisis period. In stark contrast, the upside beta ($\beta(0.95)$), originating from a similar pre-crisis baseline of 0.96, capitalized on the stimulus-fueled recovery, surging to a clear peak of 1.38. This was followed by a structural re-pricing; the beta did not return to its original level but instead established a new, markedly lower equilibrium, averaging 0.75 in the post-crisis period. The true asymmetry is therefore a dynamic sequence: a transient, symmetric risk spike followed by a powerful, asymmetric divergence. The superior stability of BSQR is what makes this nuanced, multi-phase narrative unambiguously clear.

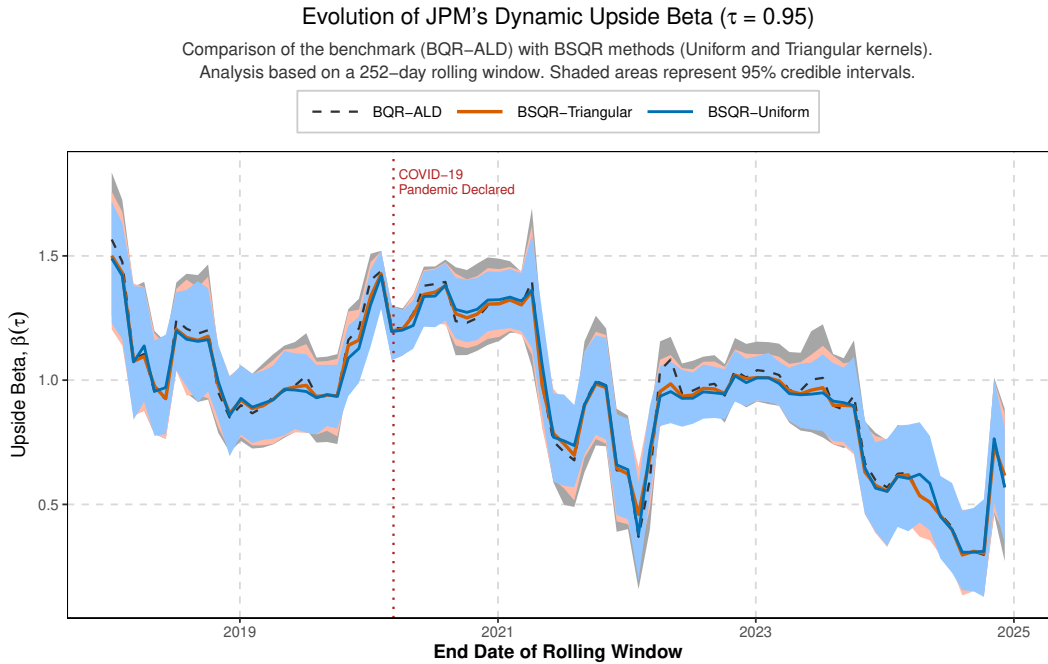
8.2 Predictive accuracy and sampler efficiency

Beyond inferential quality, we assess BSQR’s out-of-sample predictive accuracy and computational efficiency. Table 2 shows that BSQR’s predictive accuracy, measured by the average one-day-ahead check loss, is highly competitive. For the downside quantile level ($\tau = 0.05$), the performance of BSQR-Uniform (0.002998) and BSQR-Triangular (0.003031) is economically indistinguishable from BQR-ALD (0.003027). Notably, for the upside quantile level ($\tau = 0.95$), both BSQR methods (0.001338 and 0.001349) outperform the BQR-ALD benchmark (0.001363). This result is powerful: the substantial gains in inferential stability from BSQR are achieved without sacrificing—and in the upside case, even enhancing—predictive accuracy.

Computationally, Table 3 confirms BSQR’s superior sampler efficiency. This is quantified by the average minimum effective sample size (Avg. Min. ESS), where higher values indicate more reliable



(a) Evolution of the dynamic downside beta ($\beta(0.05)$) for JPM.



(b) Evolution of the dynamic upside beta ($\beta(0.95)$) for JPM.

Figure 1. Evolution of dynamic downside and upside systemic risk betas for JPM.

Note: The figures plot the posterior mean and 95% credible intervals for the (a) downside beta ($\tau = 0.05$) and (b) upside beta ($\tau = 0.95$), estimated using a 252-day rolling window. The BQR-ALD (benchmark) estimates exhibit wider and more volatile credible intervals compared to the smoother and tighter intervals from the BSQR methods.

Table 3. MCMC sampler efficiency in rolling-window analysis.

Methods	Avg. Min. ESS	Avg. Time (s)	Avg. Divergences	Avg. Selected h
BQR-ALD	1399.66	0.78	0.00	NA
BSQR-Uniform	2554.72	0.69	0.00	0.60
BSQR-Triangular	2506.05	4.39	0.01	0.66

posterior draws. The BSQR methods yield Avg. Min. ESS values (2554.72 for Uniform, 2506.05 for Triangular) that are approximately 83% and 79% higher, respectively, than for BQR-ALD (1399.66). This confirms that BSQR’s HMC-based sampler explores the posterior more effectively than BQR-ALD’s Gibbs sampler. The enhanced quality of the BSQR-Triangular method involves a higher computational time (4.39s vs. 0.78s), reflecting a clear trade-off. For applications where inferential robustness is paramount, BSQR is the superior methodological choice.

In aggregate, our empirical application demonstrates that BSQR is a significant methodological advancement. It delivers quantifiably more reliable and stable parameter estimates while maintaining competitive predictive performance. This enhanced inferential fidelity enables a more credible and nuanced understanding of economic phenomena, constituting a powerful tool for researchers and practitioners who prioritize robustness in their models.

9 Discussion

This paper introduces Bayesian smoothed quantile regression (BSQR), a framework that replaces the non-smooth check loss with a kernel-smoothed alternative. By establishing a differentiable smoothed likelihood, BSQR creates a framework that is both computationally efficient and, thanks to its proven posterior consistency, inferentially sound. Our theoretical contributions are central to this success. The formal proof of posterior consistency provides the foundational guarantee that BSQR resolves the inferential bias of standard BQR. Beyond this, our analysis of posterior propriety under various priors clarifies the validity of Bayesian inference in smoothed loss settings, and our established connection between compact-support kernels and tail equivalence with standard BQR posteriors offers key insights into the role of localization. These results suggest that similar smoothing strategies could be applied to other non-smooth Bayesian objective functions, such as in robust regression (Gelman et al., 2008) or classification with hinge loss (Polson & Scott, 2011). The ability to employ HMC and NUTS represents a computational paradigm shift for Bayesian quantile regression. The observed 20–40% improvements in effective sample size make previously intractable problems feasible, especially as models grow in complexity to include high-dimensional or hierarchical components (Reich et al., 2011; Yang & Tokdar,

2017).

Several avenues for future research are apparent, including extending the framework to multivariate settings (Hallin et al., 2010), developing dynamic models with time-varying parameters (Koop & Korobilis, 2019), and pursuing a deeper theoretical treatment of bandwidth selection (Silverman, 1986). Even with these exciting future directions, BSQR, as presented, already represents a significant advance. By smoothing the objective function rather than approximating the posterior, it maintains the coherence of the Bayesian framework while unlocking the power of modern computational tools. The rigorous proof of posterior consistency, compelling empirical evidence, and computational efficiency position BSQR as a valuable addition to the statistical toolkit. As the field grapples with increasing complexity, the principles underlying BSQR—thoughtful smoothing, guaranteed asymptotic correctness, and computational efficiency—will remain essential guideposts for both researchers and practitioners.

Declaration of competing interest

The authors declare that they have no conflict of interest.

Author contributions

Bingqi Liu conceived the study, developed the Bayesian smoothed quantile regression (BSQR) framework, derived its theoretical properties, wrote the software, and conducted all numerical experiments. He also wrote the initial draft of the manuscript. Kangqiang Li provided assistance with the proofs of asymptotic posterior consistency and kernel effects on posterior concentration. Tianxiao Pang supervised the research and provided critical feedback on the manuscript. All authors reviewed and approved the final manuscript.

Data and code availability

The source code and data required to replicate all numerical results in this paper are publicly available on GitHub at the following repository: <https://github.com/BeauquinLau/BSQR>.

References

Alhamzawi, R., & Ali, H. T. M. (2018). The Bayesian adaptive lasso regression. *Mathematical Biosciences*, 303, 75–82. doi: 10.1016/j.mbs.2018.06.004

Belloni, A., & Chernozhukov, V. (2011). ℓ_1 -penalized quantile regression in high-dimensional sparse models. *The Annals of Statistics*, 39(1), 82–130. doi: 10.1214/10-AOS827

Betancourt, M. (2017). A conceptual introduction to Hamiltonian Monte Carlo. *arXiv preprint arXiv:1701.02434*. doi: 10.48550/arXiv.1701.02434

Carpenter, B., Gelman, A., Hoffman, M. D., Lee, D., Goodrich, B., Betancourt, M., ... Riddell, A. (2017). Stan: A probabilistic programming language. *Journal of Statistical Software*, 76(1), 1–32. doi: 10.18637/jss.v076.i01

Chernozhukov, V., Fernández-Val, I., & Melly, B. (2013). Inference on counterfactual distributions. *Econometrica*, 81(6), 2205–2268. doi: 10.3982/ECTA10582

Chernozhukov, V., & Hong, H. (2003). An MCMC approach to classical estimation. *Journal of Econometrics*, 115(2), 293–346. doi: 10.1016/S0304-4076(03)00100-3

Duane, S., Kennedy, A. D., Pendleton, B. J., & Roweth, D. (1987). Hybrid Monte Carlo. *Physics Letters B*, 195(2), 216–222. doi: 10.1016/0370-2693(87)91197-X

Fan, J., & Li, R. (2001). Variable selection via nonconcave penalized likelihood and its oracle properties. *Journal of the American Statistical Association*, 96(456), 1348–1360. doi: 10.1198/016214501753382273

Fernandes, M., Guerre, E., & Horta, E. (2021). Smoothing quantile regressions. *Journal of Business & Economic Statistics*, 39(1), 338–357. doi: 10.1080/07350015.2019.1660177

Gelman, A., Jakulin, A., Pittau, M. G., & Su, Y.-S. (2008). A weakly informative default prior distribution for logistic and other regression models. *The Annals of Applied Statistics*, 2(4), 1360–1383. doi: 10.1214/08-AOAS191

Geraci, M., & Bottai, M. (2007). Quantile regression for longitudinal data using the asymmetric Laplace distribution. *Biostatistics*, 8(1), 140–154. doi: 10.1093/biostatistics/kxj039

Ghosal, S., Ghosh, J. K., & van der Vaart, A. W. (2000). Convergence rates of posterior distributions. *The Annals of Statistics*, 28(2), 500–531. doi: 10.1214/aos/1016218228

Gneiting, T. (2011). Making and evaluating point forecasts. *Journal of the American Statistical Association*, 106(494), 746–762. doi: 10.1198/jasa.2011.r10138

Hallin, M., Paindaveine, D., & Šiman, M. (2010). Multivariate quantiles and multiple-output regression quantiles: from L_1 optimization to halfspace depth. *The Annals of Statistics*, 38(2), 635–669. doi: 10.1214/09-AOS723

Hao, L., & Naiman, D. Q. (2007). *Quantile Regression*. Thousand Oaks, CA: Sage Publications, Inc. doi: 10.4135/9781412985550

Hastings, W. K. (1970). Monte Carlo sampling methods using Markov chains and their applications. *Biometrika*, 57(1), 97–109. doi: 10.2307/2334940

Hoffman, M. D., & Gelman, A. (2014). The No-U-Turn sampler: Adaptively setting path lengths in Hamiltonian Monte Carlo. *Journal of Machine Learning Research*, 15, 1593–1623. Retrieved from

<http://jmlr.org/papers/v15/hoffman14a.html>

Horowitz, J. L. (1998). *Semiparametric Methods in Econometrics* (Vol. 131). NY: Springer New York.
doi: 10.1007/978-1-4612-0621-7

Knight, K. (1998). Limiting distributions for L_1 regression estimators under general conditions. *The Annals of Statistics*, 26(2), 755–770. doi: 10.1214/aos/1028144858

Koenker, R. (2005). *Quantile Regression*. Cambridge, UK: Cambridge University Press. doi: 10.1017/CBO9780511754098

Koenker, R., & Bassett, G. (1978). Regression quantiles. *Econometrica*, 46(1), 33–50. doi: 10.2307/1913643

Koenker, R., Ng, P., & Portnoy, S. (1994). Quantile smoothing splines. *Biometrika*, 81(4), 673–680. doi: 10.2307/2337070

Koop, G., & Korobilis, D. (2019). Forecasting with high-dimensional panel VARs. *Oxford Bulletin of Economics and Statistics*, 81(5), 937–959. doi: 10.1111/obes.12303

Kozumi, H., & Kobayashi, G. (2011). Gibbs sampling methods for Bayesian quantile regression. *Journal of Statistical Computation and Simulation*, 81(11), 1565–1578. doi: 10.1080/00949655.2010.496117

Li, Q., Xi, R., & Lin, N. (2010). Bayesian regularized quantile regression. *Bayesian Analysis*, 5(3), 533–556. doi: 10.1214/10-BA521

Livingstone, S., & Zanella, G. (2019). The barker proposal: Combining robustness and efficiency in gradient-based MCMC. *Journal of the Royal Statistical Society: Series B*, 84(2), 496–523. doi: 10.1111/rssb.12482

Metropolis, N., Rosenbluth, A. W., Rosenbluth, M. N., Teller, A. H., & Teller, E. (1953). Equation of state calculations by fast computing machines. *The Journal of Chemical Physics*, 21(6), 1087–1092. doi: 10.1063/1.1699114

Neal, R. M. (2011). *MCMC Using Hamiltonian Dynamics*. NY: CRC Press. doi: 10.1201/b10905-6

Newey, W. K., & McFadden, D. (1994). Large sample estimation and hypothesis testing. In R. F. Engle & D. L. McFadden (Eds.), *Handbook of Econometrics, volume iv* (pp. 2111–2245). Elsevier. doi: 10.1016/S1573-4412(05)80005-4

Polson, N. G., & Scott, S. L. (2011). Data augmentation for support vector machines. *Bayesian Analysis*, 6(1), 1–23. doi: 10.1214/11-BA601

Portnoy, S. (1984). Asymptotic behavior of M -estimators of p regression parameters when p^2/n is large. i. consistency. *The Annals of Statistics*, 12(4), 1298–1309. doi: 10.1214/aos/1176346793

Reich, B. J., Fuentes, M., & Dunson, D. B. (2011). Bayesian spatial quantile regression. *Journal of the American Statistical Association*, 106(493), 6–20. doi: 10.1198/jasa.2010.ap09237

Salvatier, J., Wiecki, T. V., & Fonnesbeck, C. (2016). Probabilistic programming in Python using PyMC₃.

Silverman, B. W. (1986). *Density Estimation for Statistics and Data Analysis*. London: Chapman and Hall. doi: 10.1007/978-1-4899-3324-9

Sriram, K., Ramamoorthi, R. V., & Ghosh, P. (2013). Posterior consistency of Bayesian quantile regression based on the misspecified asymmetric Laplace density. *Bayesian Analysis*, 8(2), 479–504. doi: 10.1214/13-BA817

Yang, Y., & Tokdar, S. T. (2017). Joint estimation of quantile planes over arbitrary predictor spaces. *Journal of the American Statistical Association*, 112(519), 1107–1120. doi: 10.1080/01621459.2016.1192545

Yang, Y., Wang, H. J., & He, X. (2016). Posterior inference in Bayesian quantile regression with asymmetric Laplace likelihood. *International Statistical Review*, 84(3), 327–344. doi: 10.1111/insr.12114

Yu, K., & Jones, M. C. (1998). Local linear quantile regression. *Journal of the American Statistical Association*, 93(441), 228–237. doi: 10.1080/01621459.1998.10474104

Yu, K., & Moyeed, R. A. (2001). Bayesian quantile regression. *Statistics & Probability Letters*, 54(4), 437–447. doi: 10.1016/S0167-7152(01)00124-9

Appendix A: Proofs

Proof of Theorem 1. The proof follows a standard strategy for demonstrating Bayesian posterior consistency (e.g., Ghosal et al., 2000; Chernozhukov & Hong, 2003). The approach consists of two key stages: first, we establish the consistency of the frequentist M-estimator, $\hat{\beta}_h(\tau)$, which minimizes the smoothed objective function $\hat{R}_h(\mathbf{b}; \tau, h)$. Second, we leverage this result to show that the full Bayesian posterior concentrates around the true parameter value.

The M-estimator $\hat{\beta}_h(\tau)$ is the minimizer of the sample objective function Eq. (7). To prove its consistency, we analyze its population analogue, $R_h(\mathbf{b}; \tau, h) := \mathbb{E}[\hat{R}_h(\mathbf{b}; \tau, h)]$, and show that it is uniquely minimized at the true parameter $\beta_0(\tau)$ as $n \rightarrow \infty$. First, we analyze the gradient of the population objective function with respect to \mathbf{b} , which is $\nabla_{\mathbf{b}} R_h(\mathbf{b}; \tau, h) = \mathbb{E}[-\mathbf{x}_i \Psi_h(\mathbf{e}_i(\mathbf{b}); \tau)]$ by using the definition Eq. (8). Evaluating this at the true parameter $\mathbf{b} = \beta_0(\tau)$ yields:

$$\nabla_{\beta_0(\tau)} R_h(\beta_0(\tau); \tau, h) = \mathbb{E}[-\mathbf{x}_i \Psi_h(\varepsilon_{0i}; \tau)] = -\mathbb{E}_{\mathbf{x}}[\mathbf{x}_i] \cdot \mathbb{E}_{\varepsilon}[\Psi_h(\varepsilon_{0i}; \tau)],$$

where the final equality uses the independence of \mathbf{x}_i and ε_{0i} . The central task is to evaluate the expectation of the score function, $\mathbb{E}_{\varepsilon}[\Psi_h(\varepsilon_{0i}; \tau)]$, which is calculated as follows:

$$\begin{aligned} \mathbb{E}_{\varepsilon}[\Psi_h(\varepsilon_{0i}; \tau)] &= \mathbb{E}\left[\int_{-\infty}^{\infty} \psi_{\tau}(\varepsilon_{0i} - v) K_h(v) dv\right] = \int_{-\infty}^{\infty} \mathbb{E}[\tau - \mathbb{I}(\varepsilon_{0i} < v)] K_h(v) dv \\ &= \int_{-\infty}^{\infty} (\tau - F_{\varepsilon}(v)) K_h(v) dv = \int_{-\infty}^{\infty} (\tau - F_{\varepsilon}(zh)) K(z) dz. \end{aligned}$$

By **Assumption (C2a)**, $F_{\varepsilon}(u)$ is twice differentiable around 0, allowing a second-order Taylor expansion: $F_{\varepsilon}(u) = F_{\varepsilon}(0) + u f_{\varepsilon}(0) + \frac{u^2}{2} f'_{\varepsilon}(0) + o(u^2)$. Since the model definition implies $F_{\varepsilon}(0) = \tau$, we substitute $u = zh$ into the integral and obtain that

$$\begin{aligned} \mathbb{E}_{\varepsilon}[\Psi_h(\varepsilon_{0i}; \tau)] &= \int_{-\infty}^{\infty} \left(\tau - \left[\tau + (zh) f_{\varepsilon}(0) + \frac{(zh)^2}{2} f'_{\varepsilon}(0) + o((zh)^2) \right] \right) K(z) dz \\ &= -h f_{\varepsilon}(0) \int_{-\infty}^{\infty} z K(z) dz - \frac{h^2}{2} f'_{\varepsilon}(0) \int_{-\infty}^{\infty} z^2 K(z) dz + o(h^2) \\ &= 0 - O(h^2) = O(h^2) \end{aligned}$$

by utilizing $\int_{-\infty}^{\infty} z K(z) dz = 0$ in **Assumption (C4)**. Thus, $\nabla_{\beta_0(\tau)} R_h(\beta_0(\tau); \tau, h) = O(h^2)$, which converges to $\mathbf{0}$ as $n \rightarrow \infty$ due to $h \rightarrow 0$.

Next, we verify the second-order condition by examining the Hessian matrix of $R_h(\mathbf{b}; \tau, h)$ at $\beta_0(\tau)$, denoted as $\mathbf{H}_h(\beta_0(\tau))$. Note that

$$\mathbf{H}_h(\mathbf{b}) := \nabla_{\mathbf{b}}^2 R_h(\mathbf{b}; \tau, h) = \mathbb{E}[\mathbf{x}_i \mathbf{x}_i^{\top} \cdot \Psi'_h(\mathbf{e}_i(\mathbf{b}); \tau)].$$

At $\mathbf{b} = \beta_0(\tau)$, we have $\Psi'_h(\varepsilon_{0i}; \tau) = K_h(\varepsilon_{0i})$. As $n \rightarrow \infty$ and $h \rightarrow 0$, the expectation $\mathbb{E}[\Psi'_h(\varepsilon_{0i}; \tau)] = \int_{-\infty}^{\infty} K_h(u) f_{\varepsilon}(u) du$ converges to $f_{\varepsilon}(0)$. Consequently, the Hessian matrix:

$$\mathbf{H}_h(\beta_0(\tau)) \rightarrow \mathbb{E}[\mathbf{x}_i \mathbf{x}_i^{\top} f_{\varepsilon}(0)] = f_{\varepsilon}(0) \mathbb{E}[\mathbf{x}_i \mathbf{x}_i^{\top}] = f_{\varepsilon}(0) \Sigma_X.$$

This limiting matrix is positive definite, since $f_\varepsilon(0) > 0$ by **Assumption (C2a)** and Σ_X is positive definite by **Assumption (C3)**.

Since the population objective function $R_h(\mathbf{b}; \tau, h)$ has a gradient that converges to zero and a positive definite Hessian at $\beta_0(\tau)$, $\beta_0(\tau)$ is the unique minimizer of $R_h(\mathbf{b}; \tau, h)$ in the limit. To establish that $\hat{\beta}_h(\tau) \xrightarrow{P} \beta_0(\tau)$, M-estimation theory requires showing that $\sup_{\mathbf{b} \in \mathcal{B}} |\hat{R}_h(\mathbf{b}; \tau, h) - R_h(\mathbf{b}; \tau, h)| \xrightarrow{P} 0$. This uniform convergence is guaranteed by the uniform law of large numbers (ULLN), for which we must verify the existence of a dominating function for $L_h(e_i(\mathbf{b}); \tau)$ with a finite expectation. The argument of the loss function is $e_i(\mathbf{b}) = y_i - \mathbf{x}_i^\top \mathbf{b} = \varepsilon_{0i} - \mathbf{x}_i^\top (\mathbf{b} - \beta_0(\tau))$. Since the magnitude of L_h is bounded by a multiple of its argument, the task reduces to uniformly bounding $|e_i(\mathbf{b})|$ over the compact set \mathcal{B} :

$$\sup_{\mathbf{b} \in \mathcal{B}} |e_i(\mathbf{b})| \leq |\varepsilon_{0i}| + \sup_{\mathbf{b} \in \mathcal{B}} |\mathbf{x}_i^\top (\mathbf{b} - \beta_0(\tau))| \leq |\varepsilon_{0i}| + \|\mathbf{x}_i\| \sup_{\mathbf{b} \in \mathcal{B}} \|\mathbf{b} - \beta_0(\tau)\|.$$

The inequality above shows that this bound depends on two key terms, both of which are controlled by our assumptions. First, the term $\sup_{\mathbf{b} \in \mathcal{B}} \|\mathbf{b} - \beta_0(\tau)\|$ is bounded by the diameter of the parameter space, $D_{\mathcal{B}}$, because \mathcal{B} is assumed to be compact (**Assumption (C1)**). Second, the covariate norm $\|\mathbf{x}_i\|$ is uniformly bounded by a constant M_X (**Assumption (C3)**). These assumptions jointly allow us to construct a dominating function $D_i = C \cdot (|\varepsilon_{0i}| + M_X D_{\mathcal{B}})$ for some constant $C > 0$. The final condition is to ensure its expectation, $\mathbb{E}[D_i]$, is finite. This is guaranteed by **Assumption (C2b)**, which explicitly requires that the error term ε_{0i} has a finite first moment. With all conditions for the ULLN satisfied, the uniform convergence of the objective function is established. The consistency of the M-estimator, $\hat{\beta}_h(\tau) \xrightarrow{P} \beta_0(\tau)$, then follows directly from standard large-sample theory (Newey & McFadden, 1994).

With these frequentist properties established, the proof of posterior consistency follows a standard argument. The Bayesian analysis employs a quasi-likelihood function constructed from the M-estimation objective: $L(\beta, \theta | \mathbf{y}, \mathcal{X}) \propto \exp(-n\theta \hat{R}_h(\beta; \tau, h))$. The properties we have just demonstrated are precisely the conditions that ensure this quasi-likelihood concentrates its mass in a shrinking neighborhood of the true parameter. Combined with a prior distribution $\pi(\beta)$ that assigns positive mass to any such neighborhood (**Assumption (C5)**), established theorems in Bayesian asymptotics (e.g., Theorem 2.1 in Chernozhukov & Hong, 2003; see also Ghosal et al., 2000) confirm that the posterior distribution inherits this concentration property. Consequently, the posterior distribution $\pi(\beta | \mathbf{y}, \mathcal{X}, \theta)$ contracts to a point mass at the true parameter $\beta_0(\tau)$. \square

Proof of Theorem 2. Proof of Part (i). Let $I_1 = \int_{\mathbb{R}^d} L(\mathbf{y} | \mathcal{X}, \beta, \theta; \tau, h) \pi(\beta) d\beta$. From Eq. (12), we can express I_1 as:

$$I_1 \propto (Z(\theta, \tau, h))^{-n} \int_{\mathbb{R}^d} \exp(-\theta S(\beta; \tau, h)) d\beta.$$

Since $L_h(e; \tau) = (\rho_\tau * K_h)(e) \geq 0$ (due to the non-negativity of ρ_τ and K_h), it follows that $S(\beta; \tau, h) \geq 0$.

The integrand $\exp(-\theta S(\beta; \tau, h))$ is continuous and strictly positive, and $(Z(\theta, \tau, h))^{-n} > 0$, which implies $I_1 > 0$.

To establish the finiteness of I_1 , we begin by deriving a lower bound for $L_h(e; \tau)$. The check function $\rho_\tau(u)$ satisfies $\rho_\tau(u) \geq \min(\tau, 1 - \tau)|u|$. Letting $c_\tau = \min(\tau, 1 - \tau) > 0$, we obtain the following lower bound for the smoothed loss:

$$\begin{aligned} L_h(e; \tau) &= \int_{-\infty}^{\infty} \rho_\tau(e - v) K_h(v) dv \geq c_\tau \int_{-\infty}^{\infty} |e - v| K_h(v) dv \geq c_\tau \int_{-\infty}^{\infty} (|e| - |v|) K_h(v) dv \\ &= c_\tau |e| \int_{-\infty}^{\infty} K_h(v) dv - c_\tau \int_{-\infty}^{\infty} |v| K_h(v) dv = c_\tau |e| - c_\tau \int_{-\infty}^{\infty} |v| \frac{1}{h} K\left(\frac{v}{h}\right) dv \\ &= c_\tau (|e| - h M_K) \end{aligned}$$

by applying the reverse triangle inequality $|e - v| \geq |e| - |v|$ and the substitution $u = v/h$, where $M_K = \int_{-\infty}^{\infty} |u| K(u) du$ is finite by assumption. More precisely, there exist constants $c_1 = c_\tau > 0$ and $C_1 = c_\tau h M_K \geq 0$ such that $L_h(e; \tau) \geq c_1 |e| - C_1$ for all e .

Next, we derive a lower bound for $S(\beta; \tau, h)$. Summing over all observations gives

$$S(\beta; \tau, h) \geq \sum_{i=1}^n (c_1 |y_i - \mathbf{x}_i^\top \beta| - C_1) = c_1 \|\mathbf{y} - \mathbf{X}\beta\|_1 - nC_1.$$

By norm equivalence, there exists $c_2 > 0$ such that $\|z\|_1 \geq c_2 \|z\|_2$, which implies $S(\beta; \tau, h) \geq c_1 c_2 \|\mathbf{y} - \mathbf{X}\beta\|_2 - nC_1$. Using the reverse triangle inequality, we have $\|\mathbf{y} - \mathbf{X}\beta\|_2 \geq \|\mathbf{X}\beta\|_2 - \|\mathbf{y}\|_2$. Since the design matrix \mathbf{X} has full column rank d , the mapping $\beta \mapsto \mathbf{X}\beta$ is injective. This implies that $\|\mathbf{X}\beta\|_2$ defines a norm on \mathbb{R}^d . By norm equivalence on \mathbb{R}^d , there exists $c_3 > 0$ such that $\|\mathbf{X}\beta\|_2 \geq c_3 \|\beta\|_2$. Combining these, we obtain for sufficiently large $\|\beta\|_2$:

$$S(\beta; \tau, h) \geq c_1 c_2 (c_3 \|\beta\|_2 - \|\mathbf{y}\|_2) - nC_1 = (c_1 c_2 c_3) \|\beta\|_2 - (c_1 c_2 \|\mathbf{y}\|_2 + nC_1).$$

Letting $c_4 = c_1 c_2 c_3 > 0$ and $C_2 = c_1 c_2 \|\mathbf{y}\|_2 + nC_1 \geq 0$, we have the linear growth condition:

$$S(\beta; \tau, h) \geq c_4 \|\beta\|_2 - C_2.$$

This growth rate ensures the exponential decay of the integrand:

$$\exp(-\theta S(\beta; \tau, h)) \leq \exp(-\theta(c_4 \|\beta\|_2 - C_2)) = C e^{-A \|\beta\|_2},$$

where $A = \theta c_4 > 0$ and $C = e^{\theta C_2} > 0$.

To evaluate the integral $\int_{\mathbb{R}^d} e^{-A \|\beta\|_2} d\beta$, we employ d -dimensional hyperspherical coordinates. Letting $r = \|\beta\|_2$, the volume element becomes $d\beta = r^{d-1} dr d\Omega_{d-1}$, where $d\Omega_{d-1}$ is the surface element on the unit $(d-1)$ -sphere. Thus,

$$\int_{\mathbb{R}^d} e^{-A \|\beta\|_2} d\beta = \int_{\Omega_{d-1}} \int_0^\infty e^{-Ar} r^{d-1} dr d\Omega_{d-1} = \left(\int_{\Omega_{d-1}} d\Omega_{d-1} \right) \left(\int_0^\infty e^{-Ar} r^{d-1} dr \right)$$

$$= S_{d-1} \int_0^\infty e^{-Ar} r^{d-1} dr,$$

where $S_{d-1} = 2\pi^{d/2}/\Gamma(d/2)$ is the surface area of the unit $(d-1)$ -sphere. The substitution $t = Ar$ yields

$$\int_0^\infty e^{-Ar} r^{d-1} dr = \int_0^\infty e^{-t} \left(\frac{t}{A}\right)^{d-1} \frac{1}{A} dt = \frac{1}{A^d} \int_0^\infty t^{d-1} e^{-t} dt = \frac{\Gamma(d)}{A^d} = \frac{(d-1)!}{A^d},$$

since d is a positive integer. Therefore, the integral of the non-negative function $\exp(-\theta S(\beta; \tau, h))$ is

$$\int_{\mathbb{R}^d} \exp(-\theta S(\beta; \tau, h)) d\beta \leq \int_{\mathbb{R}^d} C e^{-A\|\beta\|_2} d\beta = C \int_{\mathbb{R}^d} e^{-A\|\beta\|_2} d\beta = CS_{d-1} \frac{(d-1)!}{A^d} < \infty.$$

Since $\exp(-\theta S(\beta; \tau, h))$ is non-negative and dominated by the integrable function $C e^{-A\|\beta\|_2}$, the comparison test guarantees the convergence of I_1 . Combined with the earlier result $I_1 > 0$, we conclude that $0 < I_1 < \infty$, establishing the propriety of the posterior distribution $\pi(\beta | \mathbf{y}, \mathcal{X}, \theta)$.

Proof of Part (ii). The joint posterior distribution satisfies

$$\pi(\beta, \theta | \mathbf{y}, \mathcal{X}) \propto (Z(\theta, \tau, h))^{-n} \exp(-\theta S(\beta; \tau, h)) \pi(\theta),$$

with propriety requiring the normalization integral

$$J_1 := \int_0^\infty (Z(\theta, \tau, h))^{-n} I_\beta(\theta) \pi(\theta) d\theta \tag{A.1}$$

to be finite and positive, where $I_\beta(\theta) := \int_{\mathbb{R}^d} \exp(-\theta S(\beta; \tau, h)) d\beta$. From the proof of [Theorem 2\(i\)](#), we know that there exist constants $c_L > 0$ and $C_S \geq 0$ such that $S(\beta; \tau, h) \geq c_L \|\beta\|_2 - C_S$. This yields the bound

$$\exp(-\theta S(\beta; \tau, h)) \leq \exp(-\theta(c_L \|\beta\|_2 - C_S)) = e^{\theta C_S} \exp(-\theta c_L \|\beta\|_2).$$

Hence $I_\beta(\theta)$ is dominated by

$$I_\beta(\theta) \leq e^{\theta C_S} \int_{\mathbb{R}^d} \exp(-\theta c_L \|\beta\|_2) d\beta. \tag{A.2}$$

The radial integral evaluates via hyperspherical coordinates to $\int_{\mathbb{R}^d} \exp(-\alpha \|\mathbf{x}\|_2) d\mathbf{x} = \frac{2\pi^{d/2}}{\Gamma(d/2)} \Gamma(d) \alpha^{-d}$ for $\alpha > 0$. Substituting $\alpha = \theta c_L$ we obtain the upper bound for Eq. (A.2):

$$I_\beta(\theta) \leq K_1 e^{\theta C_S} \theta^{-d}, \quad K_1 = \frac{2\pi^{d/2} \Gamma(d)}{\Gamma(d/2) c_L^d} > 0.$$

Thus, substitution into (A.1) yields the sufficient condition (15):

$$J_1 \leq K_1 \int_0^\infty \frac{\pi(\theta) e^{\theta C_S}}{(Z(\theta, \tau, h))^n \theta^d} d\theta < \infty.$$

Now, consider the specific case where the prior for θ is a Gamma distribution, $\pi(\theta) = \frac{b^a}{\Gamma(a)} \theta^{a-1} e^{-b\theta}$, for $a > 0, b > 0$. To establish the propriety of the joint posterior, it is sufficient to show that the integral

of its upper bound, as derived from the bound on $I_{\beta}(\theta)$, is finite. Let's analyze the integrand of this bounding integral:

$$\begin{aligned} \frac{\pi(\theta)e^{\theta C_S}}{(Z(\theta, \tau, h))^n \theta^d} &= \frac{b^a}{\Gamma(a)} \theta^{a-1} e^{-b\theta} \cdot \frac{e^{\theta C_S}}{(Z(\theta, \tau, h))^n \theta^d} \\ &= \frac{b^a}{\Gamma(a)} (Z(\theta, \tau, h))^{-n} \theta^{a-d-1} e^{-(b-C_S)\theta}. \end{aligned}$$

The convergence of the integral of this expression over $(0, \infty)$ depends on its asymptotic behavior as $\theta \rightarrow \infty$ and $\theta \rightarrow 0$:

1. Behavior as $\theta \rightarrow \infty$: To establish the convergence condition for large θ , we first examine the asymptotic behavior of $(Z(\theta, \tau, h))^{-n}$. This entails applying Laplace's method to $Z(\theta, \tau, h)$, which exploits the fact that, for large θ , the integrand $e^{-\theta L_h(u; \tau)}$ concentrates sharply around the global minimum of $L_h(u; \tau)$. By assumption in [Theorem 2\(ii\)](#), this minimum is $L_{\min} > 0$ and achieved at a unique point u_{\min} . The Taylor expansion of $L_h(u; \tau)$ around u_{\min} yields

$$L_h(u; \tau) = L_{\min} + \frac{L''_h(u_{\min}; \tau)}{2}(u - u_{\min})^2 + O((u - u_{\min})^3).$$

The leading asymptotic contribution to $Z(\theta, \tau, h)$ arises from integrating the exponential of the constant and quadratic terms:

$$\int_{-\infty}^{\infty} \exp\left(-\theta \left[L_{\min} + \frac{L''_h(u_{\min}; \tau)}{2}(u - u_{\min})^2\right]\right) du = e^{-\theta L_{\min}} \int_{-\infty}^{\infty} \exp\left(-\frac{\theta L''_h(u_{\min}; \tau)}{2}(u - u_{\min})^2\right) du.$$

The integral evaluates to the Gaussian form $\sqrt{2\pi/(\theta L''_h(u_{\min}; \tau))}$. Laplace's method formalizes that the full integral $Z(\theta, \tau, h)$ equals this leading term times a factor approaching 1, incorporating higher-order corrections:

$$Z(\theta, \tau, h) = \sqrt{\frac{2\pi}{L''_h(u_{\min}; \tau)}} \theta^{-1/2} e^{-\theta L_{\min}} (1 + o(1)).$$

Consequently,

$$\begin{aligned} (Z(\theta, \tau, h))^{-n} &= \left(\sqrt{\frac{2\pi}{L''_h(u_{\min}; \tau)}} \theta^{-1/2} e^{-\theta L_{\min}} (1 + o(1)) \right)^{-n} \\ &= C \cdot \theta^{n/2} e^{nL_{\min}\theta} (1 + o(1)), \end{aligned}$$

where the constant $C = (L''_h(u_{\min}; \tau)/(2\pi))^{n/2} > 0$ absorbs the prefactor, and $(1 + o(1))^{-n} = 1 + o(1)$ for fixed n . Disregarding the constant $\frac{b^a}{\Gamma(a)}$, the relevant expression becomes

$$\begin{aligned} (Z(\theta, \tau, h))^{-n} \theta^{a-d-1} e^{-(b-C_S)\theta} &= C \cdot \theta^{n/2} e^{nL_{\min}\theta} (1 + o(1)) \cdot \theta^{a-d-1} \cdot e^{-(b-C_S)\theta} \\ &= C \cdot \theta^{a+n/2-d-1} e^{-(b-C_S-nL_{\min})\theta} (1 + o(1)). \end{aligned}$$

For the integral over θ to converge as the upper limit tends to infinity, the integrand must decay. The exponential $e^{-(b-C_S-nL_{\min})\theta}$ dominates the polynomial terms for large θ , necessitating a positive coefficient for exponential decay:

$$b - C_S - nL_{\min} > 0 \implies b > C_S + nL_{\min}.$$

2. Behavior as $\theta \rightarrow 0$: Near zero, we use the assumption that $(Z(\theta, \tau, h))^{-n} = O(\theta^{k_Z})$ for some constant k_Z . The integrand's behavior is therefore dominated by the polynomial term:

$$O(\theta^{k_Z}) \cdot \theta^{a-d-1} e^{-(b-C_S)\theta} \sim O(\theta^{a+k_Z-d-1}).$$

For an integral of the form $\int_0^\epsilon \theta^p d\theta$ to converge, the exponent must satisfy $p > -1$. Applying this to our case, we require:

$$a + k_Z - d - 1 > -1 \implies a + k_Z > d.$$

Both conditions must hold simultaneously to guarantee the convergence of the bounding integral. Therefore, for a $\text{Gamma}(a, b)$ prior on θ , the joint posterior distribution $\pi(\beta, \theta | y, \mathcal{X})$ is proper if $b > C_S + nL_{\min}$ and $a + k_Z > d$. \square

Proof of Theorem 3. Proof of Part (i). The integral of interest, ignoring proportionality constants from the likelihood not involving β , is

$$I_2 := \int_{\mathbb{R}^d} \exp(-\theta S(\beta; \tau, h)) \exp\left(-\frac{\|\beta\|_2^2}{2\sigma_\beta^2}\right) d\beta.$$

Let $g(\beta) = \exp\left(-\theta S(\beta; \tau, h) - \|\beta\|_2^2/(2\sigma_\beta^2)\right)$. Since $S(\beta; \tau, h) \geq 0$ and $\theta > 0$, the term $\exp(-\theta S(\beta; \tau, h))$ is strictly positive and bounded above by 1. The Gaussian prior term $\exp(-\|\beta\|_2^2/(2\sigma_\beta^2))$ is strictly positive. Thus, $g(\beta)$ is strictly positive and continuous. Its integral over \mathbb{R}^d must therefore be strictly positive, ensuring $I_2 > 0$.

To establish finiteness, we use the comparison test. Since $-\theta S(\beta; \tau, h) \leq 0$, we have

$$-\theta S(\beta; \tau, h) - \frac{\|\beta\|_2^2}{2\sigma_\beta^2} \leq -\frac{\|\beta\|_2^2}{2\sigma_\beta^2}.$$

Exponentiating gives $g(\beta) \leq \exp\left(-\frac{\|\beta\|_2^2}{2\sigma_\beta^2}\right)$. The integral of this upper bound is $\int_{\mathbb{R}^d} \exp\left(-\frac{\|\beta\|_2^2}{2\sigma_\beta^2}\right) d\beta = (2\pi\sigma_\beta^2)^{d/2}$, which is finite. By comparison, I_2 is also finite. Thus, $0 < I_2 < \infty$, and the posterior is proper.

Proof of Part (ii). The joint posterior is proportional to

$$\pi(\beta, \theta | y, \mathcal{X}, \sigma_\beta^2, a_\theta, b_\theta) \propto (Z(\theta, \tau, h))^{-n} \exp(-\theta S(\beta; \tau, h)) \pi(\beta | \sigma_\beta^2) \pi(\theta | a_\theta, b_\theta).$$

The joint posterior density is proportional to

$$\pi(\beta, \theta | \mathbf{y}, \mathbf{X}, \sigma_\beta^2) \propto L(\mathbf{y} | \mathbf{X}, \beta, \theta) \pi(\beta | \sigma_\beta^2) \pi(\theta).$$

Substituting the likelihood form $L(\mathbf{y} | \mathbf{X}, \beta, \theta; \tau, h)$ as showed in Eq. (12), we have

$$\pi(\beta, \theta | \mathbf{y}, \mathbf{X}, \sigma_\beta^2) \propto (Z(\theta, \tau, h))^{-n} \exp(-\theta S(\beta; \tau, h)) \pi(\beta | \sigma_\beta^2) \pi(\theta).$$

To show propriety, we need to demonstrate that the integral of this joint posterior over β and θ is finite and positive:

$$J_2 := \int_0^\infty \int_{\mathbb{R}^d} (Z(\theta, \tau, h))^{-n} \exp(-\theta S(\beta; \tau, h)) \pi(\beta | \sigma_\beta^2) \pi(\theta) d\beta d\theta.$$

Since the integrand is non-negative, we can apply Tonelli's theorem to change the order of integration:

$$J_2 = \int_0^\infty (Z(\theta, \tau, h))^{-n} \pi(\theta) \left(\int_{\mathbb{R}^d} \exp(-\theta S(\beta; \tau, h)) \pi(\beta | \sigma_\beta^2) d\beta \right) d\theta.$$

Note that $\pi(\beta | \sigma_\beta^2) = (2\pi\sigma_\beta^2)^{-d/2} \exp\left(-\frac{\|\beta\|_2^2}{2\sigma_\beta^2}\right)$, so the inner integral is $(2\pi\sigma_\beta^2)^{-d/2} I_2$, where I_2 has been defined in part (i). Thus,

$$J_2 = \int_0^\infty (Z(\theta, \tau, h))^{-n} \pi(\theta) \cdot (2\pi\sigma_\beta^2)^{-d/2} I_2 d\theta.$$

From the proof of part (i) of this theorem, we established that for any fixed $\theta > 0$, $0 < I_2(\theta) < \infty$. Specifically, it was shown that $I_2(\theta) \leq \int_{\mathbb{R}^d} \exp\left(-\frac{\|\beta\|_2^2}{2\sigma_\beta^2}\right) d\beta = (2\pi\sigma_\beta^2)^{d/2}$. Substituting this inequality into the expression for J_2 :

$$0 < J_2 \leq (2\pi\sigma_\beta^2)^{-d/2} \cdot (2\pi\sigma_\beta^2)^{d/2} \int_0^\infty (Z(\theta, \tau, h))^{-n} \pi(\theta) d\theta = \int_0^\infty (Z(\theta, \tau, h))^{-n} \pi(\theta) d\theta.$$

Therefore, if the integral $\int_0^\infty (Z(\theta, \tau, h))^{-n} \pi(\theta) d\theta$ converges to a finite positive value, then J_2 is also finite and positive, ensuring the joint posterior is proper. The strict positivity of J_2 is guaranteed because $(Z(\theta, \tau, h))^{-n} > 0$, $\pi(\theta) \geq 0$ (and integrates to 1, so not identically zero), and $I_2 > 0$.

For the specific instance where $\pi(\theta | a_\theta, b_\theta)$ is a Gamma distribution with $a_\theta > 0$ and $b_\theta > 0$. The condition for propriety becomes the convergence of

$$\int_0^\infty (Z(\theta, \tau, h))^{-n} \frac{b_\theta^{a_\theta}}{\Gamma(a_\theta)} \theta^{a_\theta-1} e^{-b_\theta\theta} d\theta.$$

Since $b_\theta^{a_\theta}/\Gamma(a_\theta)$ is a positive constant, this is equivalent to the convergence of

$$\int_0^\infty (Z(\theta, \tau, h))^{-n} \theta^{a_\theta-1} e^{-b_\theta\theta} d\theta$$

to a finite positive value. \square

Proof of Proposition 1. *Proof of Part (i).* The derivative of $Z(\theta, \tau, h)$ with respect to θ is found by differentiating under the integral sign. This interchange of operations is justified by the Leibniz integral rule provided the partial derivative of the integrand is bounded in magnitude by an integrable function. For any θ in a compact interval $[a, b]$ with $0 < a < b < \infty$, we can establish such a bound:

$$\left| \frac{\partial}{\partial \theta} \exp(-\theta L_h(u; \tau)) \right| = L_h(u; \tau) \exp(-\theta L_h(u; \tau)) \leq L_h(u; \tau) \exp(-a L_h(u; \tau)).$$

The dominating function on the right-hand side is integrable on \mathbb{R} because, due to the exponential factor, it approaches zero as $|u| \rightarrow \infty$ at a rate faster than any inverse polynomial (e.g., faster than $1/u^2$). The conditions for the Leibniz rule are therefore met, and we can write:

$$\frac{\partial Z(\theta, \tau, h)}{\partial \theta} = \int_{-\infty}^{\infty} -L_h(u; \tau) \exp(-\theta L_h(u; \tau)) \, du.$$

Since $\exp(-\theta L_h(u; \tau)) > 0$ and $L_h(u; \tau)$ is non-negative and not identically zero, the integrand is non-positive and strictly negative on a set of non-zero measure. Therefore, $\partial Z(\theta, \tau, h)/\partial \theta < 0$, establishing strict decrease.

Proof of Part (ii). To show convexity of $\log Z(\theta, \tau, h)$, we examine its second derivative with respect to θ . The first-order partial derivative of $\log Z(\theta, \tau, h)$ with respect to θ is:

$$\frac{\partial \log Z(\theta, \tau, h)}{\partial \theta} = \frac{1}{Z(\theta, \tau, h)} \frac{\partial Z(\theta, \tau, h)}{\partial \theta} = \frac{\int_{-\infty}^{\infty} -L_h(u; \tau) e^{-\theta L_h(u; \tau)} \, du}{\int_{-\infty}^{\infty} e^{-\theta L_h(u; \tau)} \, du} = -\mathbb{E}_{p_u}[L_h(u; \tau)],$$

where $p_u(u \mid \theta) = \frac{\exp(-\theta L_h(u; \tau))}{Z(\theta, \tau, h)}$ can be interpreted as a probability density for u parameterized by θ .

The same justification allows for a second differentiation under the integral sign, and we have

$$\begin{aligned} & \frac{\partial^2 \log Z(\theta, \tau, h)}{\partial \theta^2} \\ &= \frac{\partial}{\partial \theta} \left(\frac{\int_{-\infty}^{\infty} -L_h(u; \tau) e^{-\theta L_h(u; \tau)} \, du}{Z(\theta, \tau, h)} \right) \\ &= \frac{\left(\int_{-\infty}^{\infty} L_h^2(u; \tau) e^{-\theta L_h(u; \tau)} \, du \right) Z(\theta, \tau, h) - \left(\int_{-\infty}^{\infty} -L_h(u; \tau) e^{-\theta L_h(u; \tau)} \, du \right) \left(\int_{-\infty}^{\infty} -L_h(u; \tau) e^{-\theta L_h(u; \tau)} \, du \right)}{Z(\theta, \tau, h)^2} \\ &= \int_{-\infty}^{\infty} L_h(u; \tau)^2 \frac{e^{-\theta L_h(u; \tau)}}{Z(\theta, \tau, h)} \, du - \left(\int_{-\infty}^{\infty} -L_h(u; \tau) \frac{e^{-\theta L_h(u; \tau)}}{Z(\theta, \tau, h)} \, du \right)^2 \\ &= \mathbb{E}_{p_u}[L_h(u; \tau)^2] - (\mathbb{E}_{p_u}[L_h(u; \tau)])^2 = \text{Var}_{p_u}(L_h(u; \tau)). \end{aligned}$$

Since variance is always non-negative, we have $\frac{\partial^2 \log Z(\theta, \tau, h)}{\partial \theta^2} \geq 0$. This confirms the convexity of $\log Z(\theta, \tau, h)$ with respect to θ . \square

Proof of Theorem 4. The posterior distributions are given by:

$$\pi_{\text{BSQR}}(\boldsymbol{\beta} \mid \theta, \mathbf{y}, \mathbf{X}; \tau, h) = \frac{1}{Z_{\text{BSQR}}(\theta, h, \pi)} \exp \left(-\theta \sum_{i=1}^n L_h(e_i(\boldsymbol{\beta}); \tau) \right) \pi(\boldsymbol{\beta}),$$

$$\pi_{\text{ALD}}(\boldsymbol{\beta} \mid \theta, \mathbf{y}, \mathbf{X}; \tau) = \frac{1}{Z_{\text{ALD}}(\theta, \pi)} \exp \left(-\theta \sum_{i=1}^n \rho_\tau(e_i(\boldsymbol{\beta})) \right) \pi(\boldsymbol{\beta}),$$

where $e_i(\boldsymbol{\beta}) = y_i - \mathbf{x}_i^\top \boldsymbol{\beta}$, and Z_{BSQR} and Z_{ALD} are the respective normalizing constants. The ratio of these posteriors is

$$\begin{aligned} R(\boldsymbol{\beta}) &:= \frac{\pi_{\text{BSQR}}(\boldsymbol{\beta} \mid \theta, h, \mathbf{y}, \mathbf{X}; \tau, h)}{\pi_{\text{ALD}}(\boldsymbol{\beta} \mid \theta, \mathbf{y}, \mathbf{X}; \tau)} = \frac{Z_{\text{ALD}}(\theta, \pi)}{Z_{\text{BSQR}}(\theta, h, \pi)} \cdot \frac{\exp(-\theta \sum_{i=1}^n L_h(e_i(\boldsymbol{\beta}); \tau)) \pi(\boldsymbol{\beta})}{\exp(-\theta \sum_{i=1}^n \rho_\tau(e_i(\boldsymbol{\beta}))) \pi(\boldsymbol{\beta})} \\ &= C_0 \cdot \exp \left(-\theta \sum_{i=1}^n [L_h(e_i(\boldsymbol{\beta}); \tau) - \rho_\tau(e_i(\boldsymbol{\beta}))] \right), \end{aligned}$$

where $C_0 = Z_{\text{ALD}}(\theta, \pi)/Z_{\text{BSQR}}(\theta, h, \pi)$ is a positive constant independent of $\boldsymbol{\beta}$. Let $\Delta_i(\boldsymbol{\beta}) = L_h(e_i(\boldsymbol{\beta}); \tau) - \rho_\tau(e_i(\boldsymbol{\beta}))$. Without loss of generality, we may re-center $K(v)$ to have zero mean, which implies the symmetry $K(v) = K(-v)$. If the initial compact support is $[a, b]$, this centering implies an effective symmetric support $[-c, c]$ where $c = (b - a)/2 > 0$, with $K(v) = 0$ for $|v| > c$. Then, from Eq. (6) with a change of variables $u = v/h$, we have $L_h(e; \tau) = \int_{-c}^c \rho_\tau(hu + e) K(u) du$. The derivative of $L_h(e; \tau) - \rho_\tau(e)$ with respect to e is

$$\frac{d}{de} [L_h(e; \tau) - \rho_\tau(e)] = \int_{-c}^c \psi_\tau(hu + e) K(u) du - \psi_\tau(e),$$

where $\psi_\tau(x) = \tau - \mathbb{I}(x < 0)$.

We first examine the case where $e > hc$ (equivalently, $e/h > c$). In this regime, for any $u \in [-c, c]$, the argument $hu + e$ satisfies $hu + e > -hc + e > -hc + hc = 0$. Consequently, $\psi_\tau(hu + e) = \tau$. Furthermore, since $e > hc > 0$, we also have $\psi_\tau(e) = \tau$. The derivative of $L_h(e; \tau) - \rho_\tau(e)$ with respect to e is therefore:

$$\frac{d}{de} [L_h(e; \tau) - \rho_\tau(e)] = \int_{-c}^c \tau K(u) du - \tau = \tau \int_{-c}^c K(u) du - \tau = 0.$$

This implies that $L_h(e; \tau) - \rho_\tau(e)$ remains constant for $e > hc$. To determine this constant value, we directly evaluate the difference:

$$L_h(e; \tau) - \rho_\tau(e) = \int_{-c}^c [\rho_\tau(hu + e) - \rho_\tau(e)] K(u) du.$$

Given $e > hc$, both $hu + e$ and e are positive. Hence, $\rho_\tau(x) = \tau x$ for $x > 0$. The integrand simplifies to $\tau(hu + e) - \tau e = \tau hu$. The integral then becomes

$$\int_{-c}^c \tau hu K(u) du = \tau h \int_{-c}^c u K(u) du = 0,$$

since $\int_{-c}^c u K(u) du = 0$ due to $K(u)$ is symmetric about 0 on its support $[-c, c]$. Therefore, for $e > hc$, it follows that $L_h(e; \tau) = \rho_\tau(e)$.

Next, we consider the case where $e < -hc$ (equivalently, $e/h < -c$). In this regime, for any $u \in [-c, c]$, the argument $hu + e$ satisfies $hu + e < hc + e < hc - hc = 0$. Consequently, $\psi_\tau(hu + e) = \tau - 1$.

Furthermore, since $e < -hc < 0$, we have $\psi_\tau(e) = \tau - 1$. The derivative of $L_h(e; \tau) - \rho_\tau(e)$ with respect to e is:

$$\frac{d}{de} [L_h(e; \tau) - \rho_\tau(e)] = \int_{-c}^c (\tau - 1) K(u) du - (\tau - 1) = (\tau - 1) \int_{-c}^c K(u) du - (\tau - 1) = 0.$$

This implies that $L_h(e; \tau) - \rho_\tau(e)$ is also constant for $e < -hc$. To determine this constant, we evaluate the difference:

$$L_h(e; \tau) - \rho_\tau(e) = \int_{-c}^c [\rho_\tau(hu + e) - \rho_\tau(e)] K(u) du.$$

Given $e < -hc$, both $hu + e$ and e are negative. Hence, $\rho_\tau(x) = (\tau - 1)x$ for $x < 0$. The integrand simplifies to $(\tau - 1)(hu + e) - (\tau - 1)e = (\tau - 1)hu$. The integral then becomes

$$\int_{-c}^c (\tau - 1)hu K(u) du = (\tau - 1)h \int_{-c}^c u K(u) du = 0.$$

Therefore, for $e < -hc$, it follows that $L_h(e; \tau) = \rho_\tau(e)$.

Based on the previous case analysis, we conclude that for residuals $e_i(\beta)$ satisfying $|e_i(\beta)/h| > c$, $\Delta_i(\beta) = 0$. For residuals $e_i(\beta)$ such that $|e_i(\beta)/h| \leq c$, $e_i(\beta)$ lies in the compact interval $[-hc, hc]$. Within this interval, $L_h(u; \tau)$ and $\rho_\tau(u)$ are continuous functions of u on $[-hc, hc]$. The continuity of $L_h(u; \tau)$ on $[-hc, hc]$ follows from the continuity of $\rho_\tau(u)$ and the properties of convolution with a well-behaved kernel $K(u)$. Thus, $\Delta_i(\beta)$ is also a continuous function of $e_i(\beta)$ over this interval. By the Extreme Value Theorem, there exist constants $m_{\text{in}}(h, \tau, c)$ and $M_{\text{in}}(h, \tau, c)$ such that for all $u \in [-hc, hc]$, $m_{\text{in}}(h, \tau, c) \leq \Delta_i(\beta) \leq M_{\text{in}}(h, \tau, c)$. Let $m_L = \min(0, m_{\text{in}}(h, \tau, c))$ and $M_U = \max(0, M_{\text{in}}(h, \tau, c))$. It follows that $m_L \leq \Delta_i(\beta) \leq M_U$ for any $e_i(\beta)$. Consequently, $\sum_{i=1}^n \Delta_i(\beta)$ is bounded as:

$$n \cdot m_L \leq \sum_{i=1}^n \Delta_i(\beta) \leq n \cdot M_U.$$

The exponential term $\exp(-\theta \sum_{i=1}^n \Delta_i(\beta))$ is therefore bounded below by $\exp(-\theta n M_U)$ and above by $\exp(-\theta n m_L)$. Thus, the ratio $R(\beta)$ satisfies:

$$C_0 \exp(-\theta n M_U) \leq R(\beta) \leq C_0 \exp(-\theta n m_L).$$

Denoting these lower and upper bounds as $M_1 = C_0 \exp(-\theta n M_U)$ and $M_2 = C_0 \exp(-\theta n m_L)$ respectively, we observe that M_1 and M_2 are positive constants independent of β . This establishes the desired result. \square

Proof of Theorem 5. We evaluate the Hessian $\mathbf{H}_L(\beta; K)$ at the true parameter $\beta_0(\tau)$. At this point, the residuals become the true errors, $e_i(\beta_0(\tau)) = \varepsilon_{0i}$, and from Eq. (16), we have

$$\mathbf{H}_L(\beta_0(\tau); K) = \frac{\theta}{h} \sum_{i=1}^n K\left(\frac{\varepsilon_{0i}}{h}\right) \mathbf{x}_i \mathbf{x}_i^\top.$$

Then, the expected Hessian is

$$\mathcal{H}_L(\beta_0(\tau); K) = \mathbb{E}_{\varepsilon_{0i} \sim f_{\varepsilon_0}, \mathbf{x}_i \sim P_{\mathbf{X}}} \left[\frac{\theta}{h} \sum_{i=1}^n K\left(\frac{\varepsilon_{0i}}{h}\right) \mathbf{x}_i \mathbf{x}_i^\top \right]$$

$$\begin{aligned}
&= \frac{\theta}{h} \sum_{i=1}^n \mathbb{E}_{\varepsilon_{0i} \sim f_{\varepsilon_0}, \mathbf{x}_i \sim P_{\mathbf{X}}} \left[K\left(\frac{\varepsilon_{0i}}{h}\right) \mathbf{x}_i \mathbf{x}_i^\top \right] \\
&= \frac{\theta}{h} \sum_{i=1}^n s_K(h) \cdot \mathbb{E}[\mathbf{x}_i \mathbf{x}_i^\top] = \frac{\theta}{h} n s_K(h) \Sigma_x
\end{aligned}$$

by using the independence of ε_{0i} and \mathbf{x}_i . The relationship between $\mathcal{H}_L(\beta_0(\tau); K_A)$ and $\mathcal{H}_L(\beta_0(\tau); K_B)$ is determined by examining their difference

$$\mathcal{H}_L(\beta_0(\tau); K_A) - \mathcal{H}_L(\beta_0(\tau); K_B) = \frac{\theta}{h} n (s_{K_A}(h) - s_{K_B}(h)) \Sigma_x.$$

The scalar term $c := \frac{\theta}{h} n (s_{K_A}(h) - s_{K_B}(h)) > 0$, since $s_{K_A}(h) - s_{K_B}(h) > 0$ by assumption, and $\theta > 0, h > 0$. Since the matrix Σ_x is positive definite by assumption, the difference is positive definite (strict Loewner order).

For the sample Hessian, the difference is $\theta/h \sum_{i=1}^n (K_A\left(\frac{\varepsilon_{0i}}{h}\right) - K_B\left(\frac{\varepsilon_{0i}}{h}\right)) \mathbf{x}_i \mathbf{x}_i^\top$, which is a sum of random matrices. By the law of large numbers, the normalized version $1/n (\mathbf{H}_L(\beta_0(\tau); K_A) - \mathbf{H}_L(\beta_0(\tau); K_B)) \xrightarrow{P} \theta/h (s_{K_A}(h) - s_{K_B}(h)) \Sigma_x > \mathbf{0}$ as $n \rightarrow \infty$, ensuring the strict inequality holds asymptotically with probability approaching 1. \square

Appendix B: Algorithms

Algorithm 1: Hamiltonian Monte Carlo sampling for β

Input: Data (\mathbf{y}, \mathbf{X}) , current precision value θ_c , quantile level τ , bandwidth h ; prior specification $\pi(\beta)$; initial state $\beta^{(0)}$; number of MCMC iterations N ; HMC leapfrog steps J ; HMC step size ϵ ; HMC mass matrix M .

Output: Markov chain samples $\{\beta^{(1)}, \dots, \beta^{(N)}\}$ approximately from $\pi(\beta \mid \theta_c, \mathbf{y}, \mathbf{X}; \tau, h)$.

for $k = 1, \dots, N$ **do**

 Let $\beta_c = \beta^{(k-1)}$;

Step 1 (Momentum Sampling):

 Draw an initial momentum $\mathbf{p}_c \sim \mathcal{N}(\mathbf{0}, M)$;

 Set $\tilde{\beta} \leftarrow \beta_c$ and $\tilde{\mathbf{p}} \leftarrow \mathbf{p}_c$;

Step 2 (Trajectory Simulation):

for $l = 1, \dots, L$ **do**

$\mathbf{p}_{\text{half}} \leftarrow \tilde{\mathbf{p}} - (\epsilon/2) \nabla_{\beta} U(\tilde{\beta} \mid \theta_c, \mathbf{y}, \mathbf{X})$;

$\tilde{\beta} \leftarrow \tilde{\beta} + \epsilon M^{-1} \mathbf{p}_{\text{half}}$;

$\tilde{\mathbf{p}} \leftarrow \mathbf{p}_{\text{half}} - (\epsilon/2) \nabla_{\beta} U(\tilde{\beta} \mid \theta_c, \mathbf{y}, \mathbf{X})$;

end

 Let the proposal be $(\beta^*, \mathbf{p}^*) = (\tilde{\beta}, \tilde{\mathbf{p}})$;

Step 3 (Metropolis Acceptance):

 Calculate acceptance probability:

$$\alpha = \min \left(1, \frac{\exp(-U(\beta^* \mid \theta_c, \mathbf{y}, \mathbf{X}) - K(\mathbf{p}^*))}{\exp(-U(\beta_c \mid \theta_c, \mathbf{y}, \mathbf{X}) - K(\mathbf{p}_c))} \right); \quad (\text{B.1})$$

 Draw $u \sim \text{Uniform}(0, 1)$;

if $u < \alpha$ **then**

 Set $\beta^{(k)} \leftarrow \beta^*$;

end

else

 Set $\beta^{(k)} \leftarrow \beta_c$;

end

end

Algorithm 2: Metropolis-Hastings sampling for θ

Input: Data (\mathbf{y}, \mathbf{X}) , current regression coefficients β_c , quantile level τ , bandwidth h ; prior parameters (a_θ, b_θ) for $\pi(\theta)$; initial state $\theta^{(0)}$; number of MCMC iterations N ; MH proposal variance $\sigma_{\log \theta}^2$.

Output: Markov chain samples $\{\theta^{(1)}, \dots, \theta^{(N)}\}$ approximately from $\pi(\theta | \beta_c, \mathbf{y}, \mathbf{X}; \tau, h)$.

for $k = 1, \dots, N$ **do**

 Let $\theta_c \leftarrow \theta^{(k-1)}$;
 Let $\beta_c \leftarrow \beta^{(k)}$ (from Algorithm 1);

Step 1 (Proposal Generation):

 Generate $z \sim \mathcal{N}(0, 1)$;
 Propose $\theta^* \leftarrow \theta_c \exp(\sigma_{\log \theta} z)$;

Step 2 (Calculate Normalizing Constants):

 Numerically evaluate $Z(\theta_c, \tau, h) = \int_{-\infty}^{\infty} \exp(-\theta_c L_h(u; \tau)) du$;
 Numerically evaluate $Z(\theta^*, \tau, h) = \int_{-\infty}^{\infty} \exp(-\theta^* L_h(u; \tau)) du$;
 ; // Requires numerical integration using the specific $L_h(u; \tau)$ for the chosen kernel.

Step 3 (Metropolis-Hastings Acceptance):

 Calculate $S(\beta_c; \tau, h) \leftarrow \sum_{i=1}^n L_h(y_i - \mathbf{x}_i^\top \beta_c; \tau)$;
 Calculate the log acceptance ratio $\log r$:

$$\begin{aligned} \log r \leftarrow & -(\theta^* - \theta_c) S(\beta_c; \tau, h) - n(\log Z(\theta^*, \tau, h) - \log Z(\theta_c, \tau, h)) \\ & + a_\theta (\log \theta^* - \log \theta_c) - b_\theta (\theta^* - \theta_c); \end{aligned}$$

 Calculate acceptance probability $\alpha \leftarrow \min(1, \exp(\log r))$;

 Draw $u \sim \text{Uniform}(0, 1)$;

if $u < \alpha$ **then**

 Set $\theta^{(k)} \leftarrow \theta^*$;

end

else

 Set $\theta^{(k)} \leftarrow \theta_c$;

end

end

Appendix C: Derivations

C.1 Gaussian kernel

From Eq. (8), we know that the smoothed loss function $L_h(e; \tau)$ can be obtained by integrating $\Psi_h(e; \tau)$ with respect to e :

$$L_h(e; \tau) = \int_{-\infty}^e \Psi_h(s; \tau) \, ds.$$

Substituting the expression of Ψ_h from Eq. (19):

$$\begin{aligned} L_h(e; \tau) &= \int_{-\infty}^e \left(\Phi\left(\frac{s}{h}\right) - (1 - \tau) \right) \, ds = \int_{-\infty}^e \Phi\left(\frac{s}{h}\right) \, ds - \int_{-\infty}^e (1 - \tau) \, ds \\ &= \int_{-\infty}^e \Phi\left(\frac{s}{h}\right) \, ds - (1 - \tau)e. \end{aligned}$$

The first integral, $\int_{-\infty}^e \Phi(s/h) \, ds$, is evaluated using integration by parts ($\int u \, dv = uv - \int v \, du$). Let $u = \Phi(s/h)$ and $dv = ds$ (so $v = s$), then $du = \frac{1}{h}\phi(s/h) \, ds$ (since $\Phi'(t) = \phi(t)$). So we have

$$\int_{-\infty}^e \Phi\left(\frac{s}{h}\right) \, ds = \left[s\Phi\left(\frac{s}{h}\right) \right]_{-\infty}^e - \int_{-\infty}^e s \cdot \frac{1}{h}\phi\left(\frac{s}{h}\right) \, ds.$$

The boundary term evaluates to $e\Phi(e/h) - \lim_{s \rightarrow -\infty} s\Phi(s/h)$. Since $\Phi(s/h) \rightarrow 0$ as $s \rightarrow -\infty$ and $s\Phi(s/h) \rightarrow 0$ (by L'Hôpital's rule or known Gaussian tail behavior), this simplifies to $e\Phi(e/h)$. Thus,

$$\int_{-\infty}^e \Phi\left(\frac{s}{h}\right) \, ds = e\Phi\left(\frac{e}{h}\right) - \frac{1}{h} \int_{-\infty}^e s\phi\left(\frac{s}{h}\right) \, ds.$$

To evaluate $\int_{-\infty}^e s\phi(s/h) \, ds$, we let $w = -s^2/(2h^2)$, then $dw = -s/h^2 \, ds$, which implies $s \, ds = -h^2 \, dw$.

The limits change: as $s \rightarrow -\infty$, $w \rightarrow -\infty$; as $s \rightarrow e$, $w \rightarrow -e^2/(2h^2)$. Thus,

$$\begin{aligned} \int_{-\infty}^e s\phi\left(\frac{s}{h}\right) \, ds &= \int_{-\infty}^e \frac{1}{\sqrt{2\pi}} e^{-s^2/(2h^2)} s \, ds = \frac{1}{\sqrt{2\pi}} \int_{-\infty}^{-e^2/(2h^2)} e^w (-h^2 \, dw) \\ &= -h^2 \frac{1}{\sqrt{2\pi}} \int_{-\infty}^{-e^2/(2h^2)} e^w \, dw = -h^2 \frac{1}{\sqrt{2\pi}} [e^w]_{-\infty}^{-e^2/(2h^2)} \\ &= -h^2 \frac{1}{\sqrt{2\pi}} \left(e^{-e^2/(2h^2)} - \lim_{w \rightarrow -\infty} e^w \right) = -h^2 \frac{1}{\sqrt{2\pi}} e^{-e^2/(2h^2)} = -h^2 \phi\left(\frac{e}{h}\right), \end{aligned}$$

since $\lim_{w \rightarrow -\infty} e^w = 0$. Substituting this back:

$$\int_{-\infty}^e \Phi\left(\frac{s}{h}\right) \, ds = e\Phi\left(\frac{e}{h}\right) - \frac{1}{h} \left(-h^2 \phi\left(\frac{e}{h}\right) \right) = e\Phi\left(\frac{e}{h}\right) + h\phi\left(\frac{e}{h}\right).$$

Combining all parts:

$$L_h(e; \tau) = e\Phi\left(\frac{e}{h}\right) + h\phi\left(\frac{e}{h}\right) - (1 - \tau)e,$$

which can be rewritten as:

$$L_h(e; \tau) = e \left(\Phi\left(\frac{e}{h}\right) - (1 - \tau) \right) + h\phi\left(\frac{e}{h}\right).$$

This derived form aligns with established results in the literature (e.g., Section 3.4 of [Koenker, 2005](#)) and satisfies $L_h(e; \tau) \rightarrow \rho_\tau(e)$ as $h \rightarrow 0$, consistent with the asymptotic properties discussed in [Horowitz \(1998\)](#).

C.2 Uniform kernel

The standard Uniform kernel is defined as $K(v) = 1/2$ for $v \in [-1, 1]$ and $K(v) = 0$ otherwise. Its corresponding CDF, $F_K(u)$, is given by:

$$F_K(u) = \begin{cases} 0 & \text{if } u < -1, \\ \frac{u+1}{2} & \text{if } -1 \leq u \leq 1, \\ 1 & \text{if } u > 1. \end{cases}$$

Substituting this CDF into the general expression for $\Psi_h(e; \tau)$ in Eq. (18), we obtain a piecewise function for $\Psi_h(e; \tau)$ with the Uniform kernel:

$$\Psi_h(e; \tau) = \begin{cases} -(1 - \tau) & \text{if } e/h < -1, \\ \frac{e}{2h} + \tau - \frac{1}{2} & \text{if } -1 \leq e/h \leq 1, \\ \tau & \text{if } e/h > 1. \end{cases}$$

The smoothed loss function $L_h(e; \tau)$ is constructed to match the pinball loss $\rho_\tau(e)$ in the outer regions where $|e/h| \geq 1$. Specifically, $L_h(e; \tau) = e(\tau - 1)$ for $e/h \leq -1$ (i.e., $e \leq -h$), and $L_h(e; \tau) = e\tau$ for $e/h \geq 1$ (i.e., $e \geq h$).

In the central region, where $-1 < e/h < 1$ (i.e., $-h < e < h$), $L_h(e; \tau)$ is obtained by integrating the corresponding segment of $\Psi_h(e; \tau)$:

$$L_h(e; \tau) = \int \left(\frac{e}{2h} + \tau - \frac{1}{2} \right) de = \frac{e^2}{4h} + e \left(\tau - \frac{1}{2} \right) + C_U,$$

where C_U is the constant of integration for this segment. To ensure continuity of $L_h(e; \tau)$ at the boundary $e = -h$, the value of the central segment's expression at $e = -h$ must equal the value from the left segment, which is $\rho_\tau(-h) = (-h)(\tau - 1) = h(1 - \tau)$. Setting these equal allows us to solve for C_U : $(-h)^2/4h + (-h) \left(\tau - \frac{1}{2} \right) + C_U = h(1 - \tau)$, we have $C_U = h/4$. Substituting it into the expression for the central segment, the complete piecewise definition of the smoothed loss function $L_h(e; \tau)$ for the Uniform kernel is:

$$L_h(e; \tau) = \begin{cases} e(\tau - 1) & \text{if } e/h \leq -1, \\ \frac{e^2}{4h} + e \left(\tau - \frac{1}{2} \right) + \frac{h}{4} & \text{if } -1 < e/h < 1, \\ e\tau & \text{if } e/h \geq 1. \end{cases}$$

This construction ensures $L_h(e; \tau)$ is continuous at $e = -h$. We now verify continuity at the other boundary, $e = h$. For the central segment evaluated at $e = h$, we have

$$L_h(h; \tau) = \frac{h^2}{4h} + h \left(\tau - \frac{1}{2} \right) + \frac{h}{4} = h\tau.$$

This value matches the expression for $L_h(e; \tau)$ in the region $e/h \geq 1$ when $e = h$, i.e., $L_h(h; \tau) = h\tau = \rho_\tau(h)$. Thus, continuity is also satisfied at $e = h$, and the derived $L_h(e; \tau)$ is continuous across all regions.

C.3 Epanechnikov kernel

The standard Epanechnikov kernel is defined by $K(v) = \frac{3}{4}(1 - v^2)$ for $v \in [-1, 1]$ and $K(v) = 0$ otherwise. Its CDF, $F_K(u)$, is piecewise:

$$F_K(u) = \begin{cases} 0 & \text{if } u < -1, \\ \frac{3}{4}u - \frac{1}{4}u^3 + \frac{1}{2} & \text{if } -1 \leq u \leq 1, \\ 1 & \text{if } u > 1. \end{cases}$$

Using this CDF in conjunction with Eq. (18), the expression for $\Psi_h(e; \tau)$ under the Epanechnikov kernel becomes:

$$\Psi_h(e; \tau) = \begin{cases} -(1 - \tau) & \text{if } e/h < -1, \\ \frac{3}{4} \left(\frac{e}{h}\right) - \frac{1}{4} \left(\frac{e}{h}\right)^3 + \tau - \frac{1}{2} & \text{if } -1 \leq e/h \leq 1, \\ \tau & \text{if } e/h > 1. \end{cases}$$

As with other kernels, the smoothed loss function $L_h(e; \tau)$ is designed to replicate the pinball loss $\rho_\tau(e)$ in the regions where $|e/h| \geq 1$. Thus, $L_h(e; \tau) = e(\tau - 1)$ for $e/h \leq -1$, and $L_h(e; \tau) = e\tau$ for $e/h \geq 1$.

For the central region, $-1 < e/h < 1$ (i.e., $-h < e < h$), $L_h(e; \tau)$ is derived by integrating the relevant segment of $\Psi_h(e; \tau)$:

$$L_h(e; \tau) = \int \left(\frac{3e}{4h} - \frac{e^3}{4h^3} + \tau - \frac{1}{2} \right) de = \frac{3e^2}{8h} - \frac{e^4}{16h^3} + e \left(\tau - \frac{1}{2} \right) + C_E,$$

where C_E is the integration constant for this segment. Continuity at the boundary $e = -h$ dictates that the value of this central expression at $e = -h$ must be equal to $\rho_\tau(-h) = (-h)(\tau - 1) = h(1 - \tau)$. This condition allows for the determination of C_E :

$$\frac{3(-h)^2}{8h} - \frac{(-h)^4}{16h^3} + (-h) \left(\tau - \frac{1}{2} \right) + C_E = h(1 - \tau),$$

which implies that $C_E = 3h/16$. Thus, the complete piecewise definition for $L_h(e; \tau)$ using the Epanechnikov kernel is:

$$L_h(e; \tau) = \begin{cases} e(\tau - 1) & \text{if } e/h \leq -1, \\ \frac{3e^2}{8h} - \frac{e^4}{16h^3} + e \left(\tau - \frac{1}{2} \right) + \frac{3h}{16} & \text{if } -1 < e/h < 1, \\ e\tau & \text{if } e/h \geq 1. \end{cases}$$

This form of $L_h(e; \tau)$ is continuous at $e = -h$ by construction. To confirm overall continuity, we check the boundary $e = h$. Evaluating the central segment at $e = h$:

$$L_h(h; \tau) = \frac{3h^2}{8h} - \frac{h^4}{16h^3} + h\left(\tau - \frac{1}{2}\right) + \frac{3h}{16} = h\tau.$$

This result, $h\tau$, matches the value of $L_h(e; \tau)$ for $e/h \geq 1$ at $e = h$ (i.e., $\rho_\tau(h)$). Therefore, the smoothed loss function $L_h(e; \tau)$ is continuous across all defined regions.

C.4 Triangular kernel

The standard Triangular kernel is given by $K(v) = 1 - |v|$ for $v \in [-1, 1]$ and $K(v) = 0$ otherwise. Its CDF, $F_K(u)$, is defined piecewise:

$$F_K(u) = \begin{cases} 0 & \text{if } u < -1, \\ \frac{1}{2}(1+u)^2 & \text{if } -1 \leq u < 0, \\ 1 - \frac{1}{2}(1-u)^2 & \text{if } 0 \leq u \leq 1, \\ 1 & \text{if } u > 1. \end{cases}$$

Substituting this CDF into Eq. (18), we derive the corresponding $\Psi_h(e; \tau)$:

$$\Psi_h(e; \tau) = \begin{cases} -(1-\tau) & \text{if } e/h < -1, \\ \frac{1}{2}\left(1 + \frac{e}{h}\right)^2 - (1-\tau) & \text{if } -1 \leq e/h < 0, \\ \tau - \frac{1}{2}\left(1 - \frac{e}{h}\right)^2 & \text{if } 0 \leq e/h \leq 1, \\ \tau & \text{if } e/h > 1. \end{cases} \quad (\text{C.1})$$

The smoothed loss function $L_h(e; \tau)$ is constructed to match the pinball loss $\rho_\tau(e)$ in the outer regions where $|e/h| \geq 1$. Thus, $L_h(e; \tau) = e(\tau - 1)$ for $e/h \leq -1$, and $L_h(e; \tau) = e\tau$ for $e/h \geq 1$.

Due to the piecewise nature of $F_K(u)$ for the Triangular kernel around $u = 0$, the central region for $L_h(e; \tau)$ ($-h < e < h$) is split into two segments. For the segment $-1 < e/h < 0$ (i.e., $-h < e < 0$), integrating the corresponding part of $\Psi_h(e; \tau)$ yields:

$$L_h(e; \tau) = \int \left(\frac{1}{2} \left(1 + \frac{e}{h}\right)^2 - (1-\tau) \right) de = \frac{h}{6} \left(1 + \frac{e}{h}\right)^3 - e(1-\tau) + C_{T1}.$$

The constant C_{T1} is determined by ensuring continuity with $\rho_\tau(e)$ at $e = -h$. Setting $L_h(-h; \tau) = \rho_\tau(-h) = h(1-\tau)$ results in $C_{T1} = 0$. Thus, for $-1 < e/h < 0$:

$$L_h(e; \tau) = \frac{h}{6} \left(1 + \frac{e}{h}\right)^3 - e(1-\tau).$$

For the segment $0 \leq e/h < 1$ (i.e., $0 \leq e < h$), integration gives:

$$L_h(e; \tau) = \int \left(\tau - \frac{1}{2} \left(1 - \frac{e}{h}\right)^2 \right) de = e\tau + \frac{h}{6} \left(1 - \frac{e}{h}\right)^3 + C_{T2}.$$

Similarly, C_{T2} is found by imposing continuity with $\rho_\tau(e)$ at $e = h$. The condition $L_h(h; \tau) = \rho_\tau(h) = h\tau$ yields $C_{T2} = 0$. Thus, for $0 \leq e/h < 1$:

$$L_h(e; \tau) = e\tau + \frac{h}{6} \left(1 - \frac{e}{h}\right)^3.$$

With $C_{T1} = 0$ and $C_{T2} = 0$, we must verify the continuity of $L_h(e; \tau)$ at the internal boundary $e = 0$: (1) As $e/h \rightarrow 0^-$, $L_h(0; \tau) = \frac{h}{6}(1+0)^3 - 0 \cdot (1-\tau) = h/6$; (2) As $e/h \rightarrow 0^+$, $L_h(0; \tau) = 0 \cdot \tau + \frac{h}{6}(1-0)^3 = h/6$. Since the limits from both sides are equal, $L_h(e; \tau)$ is continuous at $e = 0$. Combining all segments, the complete expression for $L_h(e; \tau)$ with the Triangular kernel is:

$$L_h(e; \tau) = \begin{cases} e(\tau - 1) & \text{if } e/h \leq -1, \\ \frac{h}{6} \left(1 + \frac{e}{h}\right)^3 - e(1 - \tau) & \text{if } -1 < e/h < 0, \\ e\tau + \frac{h}{6} \left(1 - \frac{e}{h}\right)^3 & \text{if } 0 \leq e/h < 1, \\ e\tau & \text{if } e/h \geq 1. \end{cases}$$

This smoothed loss function $L_h(e; \tau)$ is continuous across all regions. Furthermore, owing to the continuity of the Triangular kernel $K(v)$ itself, the derivative function $\Psi_h(e; \tau)$ given in Eq. (C.1) is also continuous for all e .

Appendix D: Simulation results

Table D. Full simulation results comparing StdQR, BQR-ALD, and our proposed BSQR with Gaussian (G), Uniform (U), Epanechnikov (E), and Triangular (T) kernels.

Error Dist.	Design	τ	Method	Estimation Accuracy (β)			Prediction	Inference (β)		Computation	MCMC Diag. (β)	
				MSE	MAE	WMSE		Coverage	CI Width		\hat{R}_{\max}	ESS _{min}
$\mathcal{N}(0, 1)$	Sparse ($p = 20$)	0.25	StdQR	0.0179	0.1072	0.2186	0.4398	—	—	—	—	—
		0.25	BQR-ALD	0.0157	0.1005	0.1928	0.7478	0.8692	0.3748	25.82	1.0021	2333.4
		0.25	BSQR-G	0.0161	0.1008	0.2061	0.4374	0.8765	0.8954	130.18	1.0060	3113.7
		0.25	BSQR-U	0.0154	0.0996	0.1900	0.4353	0.8715	0.3757	6.47	1.0019	2985.3
		0.25	BSQR-E	0.0155	0.0996	0.1901	0.4353	0.9295	0.4566	39.39	1.0020	2928.4
		0.25	BSQR-T	0.0155	0.0998	0.1905	0.4353	0.8732	0.3743	30.92	1.0019	2904.1
	Full ($p = 100$)	0.50	StdQR	0.0143	0.0950	0.1729	0.4322	—	—	—	—	—
		0.50	BQR-ALD	0.0115	0.0859	0.1404	0.4265	0.9205	0.3773	27.64	1.0021	2326.5
		0.50	BSQR-G	0.0109	0.0817	0.1399	0.4254	0.9350	0.8896	129.38	1.0060	3258.2
		0.50	BSQR-U	0.0107	0.0829	0.1307	0.4246	0.9300	0.3713	6.45	1.0019	3111.8
		0.50	BSQR-E	0.0105	0.0822	0.1286	0.4242	0.9855	0.5510	37.72	1.0019	3034.8
		0.50	BSQR-T	0.0110	0.0841	0.1348	0.4253	0.9258	0.3734	30.65	1.0019	3006.9
	Large ($p = 500$)	0.75	StdQR	0.0181	0.1065	0.2233	0.4424	—	—	—	—	—
		0.75	BQR-ALD	0.0154	0.0989	0.1909	0.7496	0.8652	0.3763	26.25	1.0021	2339.5
		0.75	BSQR-G	0.0166	0.0998	0.2239	0.4399	0.8782	0.8964	125.60	1.0060	3104.5

Continued on next page

Table D. – *Continued from previous page*

Error Dist.	Design	τ	Method	Estimation Accuracy (β)			Prediction	Inference (β)		Computation	MCMC Diag. (β)	
				MSE	MAE	WMSE		Coverage	CI Width		\hat{R}_{\max}	ESS _{min}
Normal	Uniform	0.75	BSQR-U	0.0151	0.0979	0.1874	0.4360	0.8712	0.3775	6.38	1.0020	3022.6
			BSQR-E	0.0151	0.0981	0.1878	0.4361	0.9305	0.4503	39.69	1.0019	2963.9
			BSQR-T	0.0152	0.0982	0.1881	0.4362	0.8675	0.3759	31.28	1.0019	2946.9
	Dense ($p = 8$)	0.25	StdQR	0.0159	0.1005	0.0808	0.4145	—	—	—	—	—
			BQR-ALD	0.0142	0.0951	0.0725	0.7915	0.8625	0.3570	10.08	1.0018	2174.8
			BSQR-G	0.0136	0.0933	0.0699	0.4127	0.8850	0.3665	85.94	1.0015	2804.2
			BSQR-U	0.0137	0.0932	0.0698	0.4126	0.8694	0.3558	4.27	1.0016	2734.7
			BSQR-E	0.0136	0.0929	0.0697	0.4126	0.9362	0.4378	25.87	1.0015	2722.6
			BSQR-T	0.0138	0.0935	0.0705	0.4127	0.8638	0.3554	20.39	1.0017	2705.3
	Sparse ($p = 100$)	0.50	StdQR	0.0129	0.0902	0.0651	0.4108	—	—	—	—	—
			BQR-ALD	0.0109	0.0825	0.0555	0.4092	0.9088	0.3568	10.09	1.0018	2186.0
			BSQR-G	0.0111	0.0776	0.0804	0.4110	0.9269	0.8671	88.83	1.0058	2842.0
			BSQR-U	0.0098	0.0779	0.0501	0.4081	0.9150	0.3514	4.28	1.0016	2751.5
			BSQR-E	0.0099	0.0781	0.0502	0.4081	0.9800	0.5039	24.98	1.0016	2722.8
			BSQR-T	0.0102	0.0795	0.0520	0.4085	0.9138	0.3534	20.30	1.0017	2732.6
	Sparse ($p = 1000$)	0.75	StdQR	0.0167	0.1032	0.0850	0.4156	—	—	—	—	—
			BQR-ALD	0.0152	0.0980	0.0769	0.7913	0.8494	0.3585	10.03	1.0018	2164.1
			BSQR-G	0.0147	0.0969	0.0747	0.4135	0.8700	0.3660	84.97	1.0016	2822.5
			BSQR-U	0.0145	0.0963	0.0737	0.4133	0.8588	0.3575	4.30	1.0017	2777.2

Continued on next page

Table D. – *Continued from previous page*

Error Dist.	Design	τ	Method	Estimation Accuracy (β)			Prediction	Inference (β)		Computation	MCMC Diag. (β)	
				MSE	MAE	WMSE		Coverage	CI Width		\hat{R}_{\max}	ESS _{min}
$t(3)$	Sparse ($p = 20$)	0.75	BSQR-E	0.0146	0.0963	0.0740	0.4134	0.9138	0.4276	25.69	1.0016	2730.7
		0.75	BSQR-T	0.0146	0.0966	0.0743	0.4135	0.8525	0.3565	20.39	1.0016	2729.3
		0.25	StdQR	0.0238	0.1228	0.2905	0.6021	—	—	—	—	—
		0.25	BQR-ALD	0.0212	0.1159	0.2601	1.0805	0.9022	0.4859	23.25	1.0021	2347.4
		0.25	BSQR-G	0.0215	0.1169	0.2657	0.5982	0.9118	0.5085	115.82	1.0019	3043.3
	Uniform ($p = 20$)	0.25	BSQR-U	0.0215	0.1167	0.2642	0.5979	0.9058	0.4929	6.29	1.0020	2938.7
		0.25	BSQR-E	0.0214	0.1166	0.2640	0.5979	0.9432	0.5650	39.01	1.0020	2905.6
		0.25	BSQR-T	0.0213	0.1162	0.2618	0.5975	0.9048	0.4897	30.24	1.0019	2907.8
		0.50	StdQR	0.0190	0.1096	0.2326	0.5905	—	—	—	—	—
		0.50	BQR-ALD	0.0156	0.0995	0.1910	0.5837	0.9468	0.4874	23.64	1.0022	2363.2
ζ	Sparse ($p = 20$)	0.50	BSQR-G	0.0153	0.0987	0.1889	0.5832	0.9570	0.5026	115.96	1.0019	3169.1
		0.50	BSQR-U	0.0154	0.0987	0.1887	0.5832	0.9530	0.4960	6.35	1.0020	3112.6
		0.50	BSQR-E	0.0153	0.0984	0.1881	0.5831	0.9915	0.7114	38.36	1.0019	3058.0
		0.50	BSQR-T	0.0154	0.0987	0.1886	0.5832	0.9502	0.4912	29.51	1.0020	2996.5
		0.75	StdQR	0.0241	0.1230	0.2940	0.5991	—	—	—	—	—
	Uniform ($p = 20$)	0.75	BQR-ALD	0.0221	0.1176	0.2690	1.0923	0.9030	0.4929	23.40	1.0020	2332.6
		0.75	BSQR-G	0.0241	0.1210	0.3165	0.6003	0.9112	1.0306	119.20	1.0059	3031.9
		0.75	BSQR-U	0.0225	0.1186	0.2741	0.5961	0.9008	0.4995	6.33	1.0019	2925.5
		0.75	BSQR-E	0.0225	0.1184	0.2736	0.5960	0.9410	0.5708	39.56	1.0019	2910.4

Continued on next page

Table D. – *Continued from previous page*

Error Dist.	Design	τ	Method	Estimation Accuracy (β)			Prediction	Inference (β)		Computation	MCMC Diag. (β)	
				MSE	MAE	WMSE		Coverage	CI Width		\hat{R}_{\max}	ESS _{min}
		0.75	BSQR-T	0.0223	0.1181	0.2713	0.5957	0.9010	0.4966	30.47	1.0019	2907.0
S _p	Dense ($p = 8$)	0.25	StdQR	0.0194	0.1121	0.1018	0.5687	—	—	—	—	—
		0.25	BQR-ALD	0.0176	0.1067	0.0919	1.1289	0.9006	0.4436	9.79	1.0017	2225.9
		0.25	BSQR-G	0.0181	0.1084	0.0937	0.5672	0.9106	0.4677	79.16	1.0016	2779.1
		0.25	BSQR-U	0.0180	0.1082	0.0931	0.5672	0.9050	0.4535	4.16	1.0015	2735.0
		0.25	BSQR-E	0.0179	0.1078	0.0926	0.5671	0.9525	0.5490	24.63	1.0016	2701.2
		0.25	BSQR-T	0.0177	0.1074	0.0919	0.5669	0.9025	0.4488	21.69	1.0070	2705.1
S _p	Dense ($p = 8$)	0.50	StdQR	0.0149	0.0969	0.0756	0.5651	—	—	—	—	—
		0.50	BQR-ALD	0.0129	0.0907	0.0657	0.5635	0.9488	0.4418	10.04	1.0017	2248.7
		0.50	BSQR-G	0.0126	0.0900	0.0637	0.5632	0.9556	0.4612	77.73	1.0015	2811.1
		0.50	BSQR-U	0.0126	0.0897	0.0639	0.5632	0.9550	0.4526	4.29	1.0016	2757.1
		0.50	BSQR-E	0.0125	0.0896	0.0634	0.5632	0.9931	0.6434	24.30	1.0016	2753.5
		0.50	BSQR-T	0.0127	0.0900	0.0644	0.5633	0.9531	0.4466	19.91	1.0015	2734.2
S _p	Dense ($p = 8$)	0.75	StdQR	0.0193	0.1093	0.0956	0.5660	—	—	—	—	—
		0.75	BQR-ALD	0.0182	0.1052	0.0894	1.1368	0.9069	0.4495	9.77	1.0017	2221.7
		0.75	BSQR-G	0.0188	0.1065	0.0924	0.5655	0.9181	0.4746	78.23	1.0015	2797.0
		0.75	BSQR-U	0.0186	0.1060	0.0912	0.5653	0.9088	0.4597	4.20	1.0016	2757.2
		0.75	BSQR-E	0.0184	0.1057	0.0908	0.5652	0.9475	0.5398	24.79	1.0016	2734.1

Continued on next page

Table D. – *Continued from previous page*

Error Dist.	Design	τ	Method	Estimation Accuracy (β)			Prediction	Inference (β)		Computation	MCMC Diag. (β)	
				MSE	MAE	WMSE		Coverage	CI Width		\hat{R}_{\max}	ESS _{min}
		0.75	BSQR-T	0.0183	0.1053	0.0901	0.5651	0.9088	0.4541	19.84	1.0015	2686.3
0.2 $\mathcal{N}(0, 3)$ +0.8 $\mathcal{N}(0, 4)$	Sparse ($p = 20$)	0.25	StdQR	0.0697	0.2130	0.8426	0.8584	—	—	—	—	—
		0.25	BQR-ALD	0.0611	0.1987	0.7334	1.4624	0.8622	0.7370	25.16	1.0021	2310.5
		0.25	BSQR-G	0.0617	0.1982	0.7641	0.8500	0.8788	1.2841	108.02	1.0060	3002.9
		0.25	BSQR-U	0.0600	0.1965	0.7191	0.8468	0.8650	0.7391	6.25	1.0020	2985.0
		0.25	BSQR-E	0.0601	0.1968	0.7209	0.8470	0.9288	0.9021	38.29	1.0019	2872.8
		0.25	BSQR-T	0.0603	0.1971	0.7233	0.8472	0.8645	0.7367	29.84	1.0020	2831.8
0.5 $\mathcal{N}(0, 3)$ +0.5 $\mathcal{N}(0, 4)$	Sparse ($p = 20$)	0.50	StdQR	0.0528	0.1841	0.6408	0.8402	—	—	—	—	—
		0.50	BQR-ALD	0.0426	0.1654	0.5161	0.8280	0.9295	0.7383	25.10	1.0022	2305.9
		0.50	BSQR-G	0.0373	0.1548	0.4516	0.8217	0.9418	0.7268	104.16	1.0019	3201.8
		0.50	BSQR-U	0.0394	0.1590	0.4763	0.8240	0.9342	0.7276	6.23	1.0020	3054.5
		0.50	BSQR-E	0.0387	0.1577	0.4691	0.8233	0.9912	1.0776	37.75	1.0019	3008.8
		0.50	BSQR-T	0.0409	0.1621	0.4946	0.8257	0.9318	0.7318	29.59	1.0019	2938.1
0.7 $\mathcal{N}(0, 3)$ +0.3 $\mathcal{N}(0, 4)$	Sparse ($p = 20$)	0.75	StdQR	0.0696	0.2102	0.8306	0.8542	—	—	—	—	—
		0.75	BQR-ALD	0.0591	0.1946	0.7104	1.4533	0.8660	0.7298	25.00	1.0022	2326.3
		0.75	BSQR-G	0.0590	0.1946	0.7101	0.8432	0.8858	0.7632	107.22	1.0020	3061.8
		0.75	BSQR-U	0.0584	0.1937	0.7016	0.8425	0.8705	0.7327	6.27	1.0019	2953.9
		0.75	BSQR-E	0.0585	0.1938	0.7031	0.8426	0.9302	0.8741	38.83	1.0019	2895.6
		0.75	BSQR-T	0.0585	0.1937	0.7026	0.8426	0.8712	0.7302	29.77	1.0019	2872.8

Continued on next page

Table D. – *Continued from previous page*

Error Dist.	Design	τ	Method	Estimation Accuracy (β)			Prediction	Inference (β)		Computation	MCMC Diag. (β)	
				MSE	MAE	WMSE		Coverage	CI Width		\hat{R}_{\max}	ESS _{min}
5	Dense ($p = 8$)	0.25	StdQR	0.0632	0.1993	0.3103	0.8032	—	—	—	—	—
		0.25	BQR-ALD	0.0572	0.1902	0.2807	1.5346	0.8562	0.6967	10.48	1.0019	2168.1
		0.25	BSQR-G	0.0547	0.1854	0.2725	0.7997	0.8781	0.7278	68.93	1.0015	2767.7
		0.25	BSQR-U	0.0545	0.1851	0.2706	0.7995	0.8675	0.6971	4.08	1.0017	2714.3
		0.25	BSQR-E	0.0548	0.1856	0.2713	0.7995	0.9206	0.8624	24.22	1.0016	2720.2
		0.25	BSQR-T	0.0552	0.1865	0.2726	0.7997	0.8569	0.6937	19.06	1.0015	2650.1
	Uniform ($p = 8$)	0.50	StdQR	0.0479	0.1730	0.2431	0.8006	—	—	—	—	—
		0.50	BQR-ALD	0.0411	0.1610	0.2075	0.7972	0.9125	0.6870	10.46	1.0017	2158.1
		0.50	BSQR-G	0.0356	0.1502	0.1798	0.7945	0.9319	0.6785	70.28	1.0015	2788.8
		0.50	BSQR-U	0.0376	0.1542	0.1905	0.7955	0.9238	0.6762	4.09	1.0015	2755.2
		0.50	BSQR-E	0.0377	0.1543	0.1904	0.7955	0.9812	0.9773	23.71	1.0016	2736.7
		0.50	BSQR-T	0.0390	0.1569	0.1971	0.7961	0.9150	0.6789	19.10	1.0015	2717.1
	Sparse ($p = 8$)	0.75	StdQR	0.0608	0.1966	0.3079	0.8060	—	—	—	—	—
		0.75	BQR-ALD	0.0538	0.1841	0.2737	1.5343	0.8538	0.6905	10.30	1.0018	2164.7
		0.75	BSQR-G	0.0520	0.1807	0.2634	0.8020	0.8825	0.7180	68.42	1.0016	2756.3
		0.75	BSQR-U	0.0519	0.1808	0.2620	0.8018	0.8650	0.6886	4.05	1.0017	2727.4
		0.75	BSQR-E	0.0519	0.1805	0.2631	0.8019	0.9150	0.8209	23.91	1.0016	2716.6
		0.75	BSQR-T	0.0523	0.1813	0.2658	0.8021	0.8612	0.6874	18.66	1.0015	2684.5

Continued on next page

Table D. – *Continued from previous page*

Error Dist.	Design	τ	Method	Estimation Accuracy (β)			Prediction	Inference (β)		Computation	MCMC Diag. (β)	
				MSE	MAE	WMSE		Coverage	CI Width		\hat{R}_{\max}	ESS _{min}
$\mathcal{N}(0, \sigma_i^2)$, $\sigma_i = \exp(-0.25 + 0.5x_{i1})$	Sparse ($p = 20$)	0.25	StdQR	0.0096	0.0779	0.1177	0.3824	—	—	—	—	—
		0.25	BQR-ALD	0.0089	0.0749	0.1091	0.6951	0.9190	0.3203	23.56	1.0020	2345.5
		0.25	BSQR-G	0.0091	0.0759	0.1124	0.3813	0.9178	0.3294	131.95	1.0019	2997.0
		0.25	BSQR-U	0.0091	0.0756	0.1117	0.3811	0.9145	0.3237	6.50	1.0019	2864.6
		0.25	BSQR-E	0.0091	0.0755	0.1115	0.3811	0.9508	0.3696	40.88	1.0020	2843.0
		0.25	BSQR-T	0.0090	0.0754	0.1108	0.3809	0.9145	0.3221	32.05	1.0020	2834.2
	Full ($p = 100$)	0.50	StdQR	0.0075	0.0689	0.0932	0.3760	—	—	—	—	—
		0.50	BQR-ALD	0.0064	0.0637	0.0800	0.3727	0.9502	0.3133	23.57	1.0021	2313.6
		0.50	BSQR-G	0.0076	0.0654	0.1130	0.3768	0.9538	0.8367	134.71	1.0060	3120.5
		0.50	BSQR-U	0.0064	0.0636	0.0801	0.3728	0.9515	0.3169	6.52	1.0019	3050.4
		0.50	BSQR-E	0.0064	0.0636	0.0801	0.3728	0.9915	0.4408	38.72	1.0019	3007.1
		0.50	BSQR-T	0.0064	0.0634	0.0795	0.3726	0.9512	0.3148	33.26	1.0020	2946.8
	Large ($p = 500$)	0.75	StdQR	0.0100	0.0798	0.1220	0.3823	—	—	—	—	—
		0.75	BQR-ALD	0.0091	0.0760	0.1113	0.6893	0.9062	0.3151	23.38	1.0021	2332.7
		0.75	BSQR-G	0.0092	0.0766	0.1136	0.3804	0.9095	0.3243	133.81	1.0020	3007.0
		0.75	BSQR-U	0.0092	0.0764	0.1129	0.3802	0.9050	0.3187	6.43	1.0020	2906.1
		0.75	BSQR-E	0.0092	0.0764	0.1131	0.3803	0.9405	0.3598	39.83	1.0019	2815.8
		0.75	BSQR-T	0.0091	0.0762	0.1123	0.3801	0.9062	0.3173	31.65	1.0019	2837.4

Table D. – *Continued from previous page*

Error Dist.	Design	τ	Method	Estimation Accuracy (β)			Prediction	Inference (β)		Computation	MCMC Diag. (β)	
				MSE	MAE	WMSE		Coverage	CI Width		\hat{R}_{\max}	ESS _{min}
5	Dense ($p = 8$)	0.25	StdQR	0.0086	0.0728	0.0440	0.3655	—	—	—	—	—
		0.25	BQR-ALD	0.0081	0.0704	0.0417	0.7278	0.8838	0.2887	9.76	1.0017	2221.1
		0.25	BSQR-G	0.0104	0.0739	0.0732	0.3685	0.8900	0.8085	92.17	1.0057	2805.3
		0.25	BSQR-U	0.0083	0.0710	0.0427	0.3652	0.8906	0.2939	4.33	1.0017	2759.1
		0.25	BSQR-E	0.0083	0.0709	0.0426	0.3652	0.9331	0.3454	26.41	1.0017	2729.9
		0.25	BSQR-T	0.0082	0.0705	0.0421	0.3651	0.8888	0.2912	20.92	1.0016	2744.6
	Uniform ($p = 8$)	0.50	StdQR	0.0065	0.0649	0.0338	0.3613	—	—	—	—	—
		0.50	BQR-ALD	0.0057	0.0605	0.0299	0.3602	0.9419	0.2861	9.76	1.0018	2251.1
		0.50	BSQR-G	0.0055	0.0593	0.0288	0.3600	0.9544	0.2960	95.94	1.0015	2842.0
		0.50	BSQR-U	0.0055	0.0595	0.0289	0.3600	0.9500	0.2903	4.40	1.0016	2788.6
		0.50	BSQR-E	0.0055	0.0595	0.0289	0.3600	0.9894	0.3952	25.76	1.0015	2756.1
		0.50	BSQR-T	0.0055	0.0595	0.0288	0.3599	0.9450	0.2883	24.58	1.0016	2776.2
	Sparse ($p = 8$)	0.75	StdQR	0.0083	0.0725	0.0417	0.3618	—	—	—	—	—
		0.75	BQR-ALD	0.0073	0.0683	0.0373	0.7194	0.9062	0.2865	9.65	1.0018	2228.6
		0.75	BSQR-G	0.0076	0.0695	0.0385	0.3610	0.9106	0.2969	91.77	1.0015	2801.1
		0.75	BSQR-U	0.0076	0.0693	0.0384	0.3610	0.9075	0.2913	4.33	1.0016	2764.9
		0.75	BSQR-E	0.0075	0.0692	0.0383	0.3609	0.9431	0.3373	25.99	1.0017	2729.0

0.75	BSQR-T	0.0074	0.0687	0.0378	0.3608	0.9081	0.2891	25.52	1.0015	2726.5
------	--------	---------------	---------------	---------------	---------------	--------	--------	-------	---------------	--------

Note: **Bold** values indicate superior performance among the Bayesian methods (BQR-ALD and BSQR variants) for key metrics (lower is better for MSE, MAE, WMSE, check loss, CI width, time; for coverage, closer to 0.95 is better; for \hat{R}_{\max} , closer to 1.0 is better; for ESS_{\min} , higher is better). The MCMC diagnostics reported are the maximum potential scale reduction factor (\hat{R}_{\max}) and the minimum bulk effective sample size (ESS_{\min}) across all β coefficients. For our BSQR methods, the average number of divergent transitions per replication was low (consistently below 2) and did not appear to compromise the posterior estimates.